AD-A037 591 DEFENCE RESEARCH ESTABLISHMENT OTTAWA (ONTARIO) F/G 6/18
FIELD READER FOR A COMBINED NEUTRON/GAMMA THERMOLUMINESCENT DOS--ETC(U)
FEB 77 S MCGOWAN

UNCLASSIFIED DREO-TN-76-30 NL

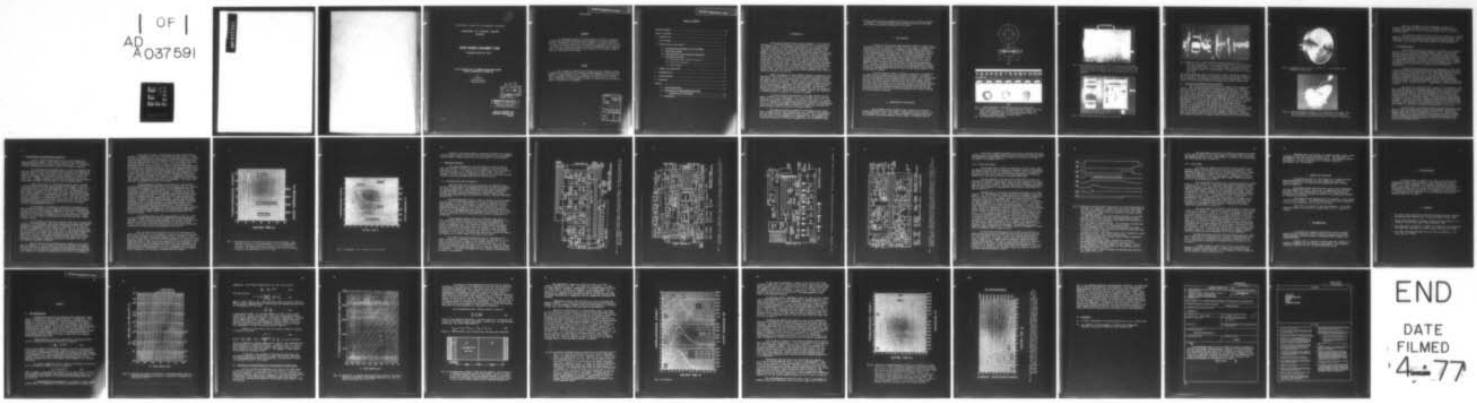

END

DATE FILMED
4-77

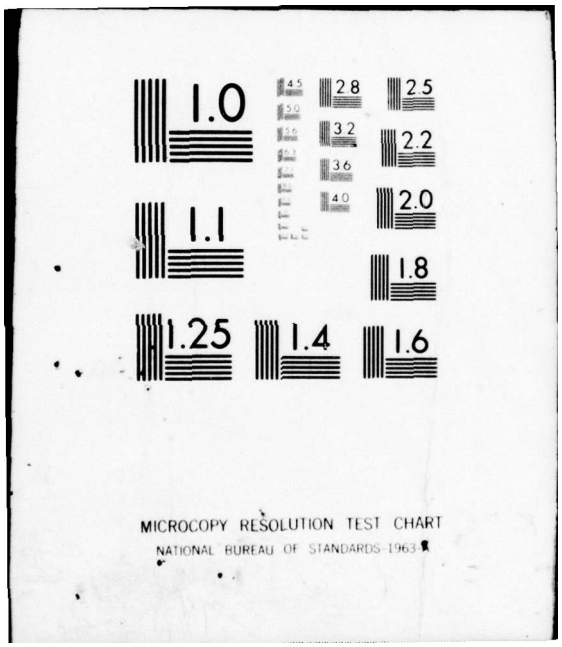
1.0
1.1
1.25
1.4
1.6
2.0
2.2
2.5
2.8
3.2
3.6
4.0
4.5
5.0
5.6
MICROCOPY RESOLUTION TEST CHART
NATIONAL BUREAU OF STANDARDS-1963

ADA037591

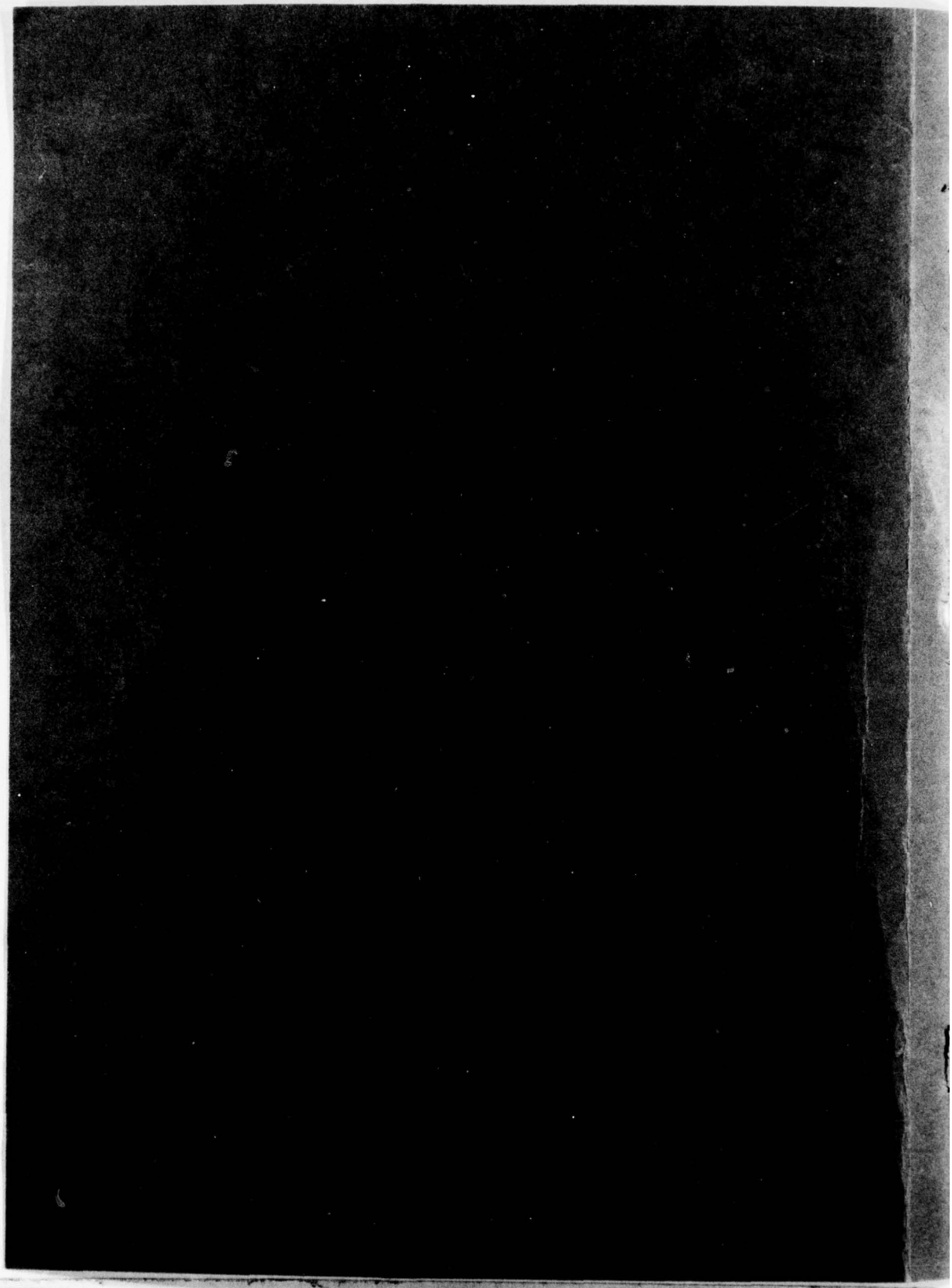

(3)

RESEARCH AND DEVELOPMENT BRANCH

DEPARTMENT OF NATIONAL DEFENCE
CANADA

DEFENCE RESEARCH ESTABLISHMENT OTTAWA

TECHNICAL NOTE NO. 76-30

FIELD READER FOR A COMBINED NEUTRON/GAMMA THERMOLUMINESCENT DOSIMETER

by

S. McGowan

Nuclear Effects Section
NBC Defence Division

DDC
RECEIVED
APR 1 1977
A

DISTRIBUTION STATEMENT A
Approved for public release;
Distribution Unlimited

RECEIVED DECEMBER 1976
PUBLISHED FEBRUARY 1977
OTTAWA

PRECEDING PAGE BLANK-NOT FILMED

ABSTRACT

An experimental model of a field reader to be used to interpret a combined neutron/gamma thermoluminescent dosimeter for military personnel has been designed and constructed. This instrument can operate from the 24-V battery of a military vehicle and can read dose to personnel in the range of 1 to 1000 rads. Satisfactory operation has been demonstrated and it has been shown that no serious limitations on the accuracy of the dosimetry measurements are introduced by the reader.

RESUME

On a conçue et construit un prototype de lecteur portatif servant à interpréter les données d'un dosimétre thermoluminescent combiné (neutron/gamma) à l'usage des militaires. L'appareil est alimenté par la batterie de 24V d'un véhicule militaire et peut indiquer une dose allant de 1 à 1000 rads. L'expérience a été concluante, de plus, le lecteur ne nuit pas sérieusement à la précision du dosiémétre.

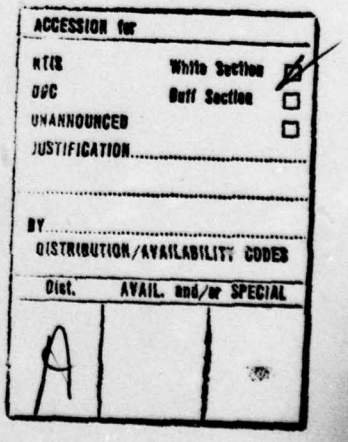

PRECEDING PAGE BLANK-NOT FILMED

TABLE OF CONTENTS

1. INTRODUCTION

The present Canadian Forces personal dosimeter (1) for ionizing radiations is the DT/60A phosphate glass dosimeter which is interpreted by the CP95A/PD reader. This dosimeter system measures the accumulated dose from gamma radiation but has a very low response to fast neutrons. While exposure to fast neutrons is considerably less probable than exposure to gammas, a sub-lethal dose composed of fast neutrons and gammas of comparable proportions could be received by military personnel at the time of burst of a small nuclear weapon (2). In fact, where some protection is provided against blast and thermal effects and there also may be appreciable gamma attenuation, such as in an armoured vehicle, neutron radiation can be the prime cause of death and injury. Thus, a dosimetry system which can measure equivalently the effective dose to personnel from gammas and fast neutrons is desired. Furthermore, since a large proportion of the radiations from a nuclear weapon is emitted in a very short time, the dosimeter must have a response faster than the conventional quartz-fibre dosimeter which relies on conduction through an ionized gas.

Recent developments of some dosimetry systems for gammas and fast neutrons involve the addition of a fast-neutron-sensitive diode to the phosphate glass. Both types of dosimeter must be read and independent neutron and gamma readings are obtained. However, since for criticality it is the total dose that is significant, a single combined reading would be sufficient for military purposes. Dosimeters are under development at DREO (3) which give a combined neutron/gamma dose in a single reading. The sensitive material is a thermoluminescent phosphor in powder form which is embedded in a hydrogenous material. Excitation of the phosphor results from ionization by knock-on protons in addition to ionization by gammas.

A military dosimetry system based on the DREO combined neutron/gamma dosimeter can be practicable only if such dosimeter can be read conveniently in a military environment. The purpose of this task is to demonstrate the feasibility of interpreting, under field conditions, the absorbed dose of a combined neutron/gamma thermoluminescent dosimeter, by designing and constructing an instrument which is capable of reading such dosimeters and which can operate from the battery of a military vehicle.

The primary objectives considered in the design of this reader were: reading accuracy, short reading time, easy interface of the dosimeter with the reader and low consumption of battery energy. Some consideration was also given to the instrument size, ruggedness, cost of components and construction and ease of servicing, although this is an experimental model

and such factors are often greatly altered when a more advanced instrument is designed. The extent to which these objectives were met is discussed below under the detailed description of the reader.

2. THE DOSIMETER

Details of the most successful dosimeter design are shown in Fig. 1. The phosphor, $CaSO_4$:Tm, $CaSO_4$:Sm, or $CaSO_4$:Dy in the form of a powder of particles about 10 μm in diameter, is embedded in cross-linked polyethylene ($(CH_2)n$) which was chosen because of its high hydrogen content and because of its high-temperature softening point. Cross-linked polyethylene softens at about 250°C compared with about 130°C for ordinary polyethylene. One part phosphor by weight is mixed with about 10 parts polyethylene and the resultant matrix is sandwiched between 25-μm Kapton tape or mica. These phosphors luminesce with a main peak at about 200°C so that, as will be explained later, the matrix will be subjected to temperatures approaching 300°C. The mica or Kapton serve both to give the matrix mechanical support, particularly during heating, and to protect the polyethylene from the atmosphere since light-emitting oxidation is found to occur during readout if the polyethylene is exposed.

The thin sandwich, which is typically 0.5 mm thick, is supported by washers which for small quantities are made of Plexiglas. The Kapton tape has the advantage of having better adhesion than mica to the polyethylene, but it can be used only with a phosphor which emits yellow light, such as $CaSO_4$:Sm. Extraneous emission from the heater and other exposed surfaces has been found to be larger in the yellow and red and can be reduced considerably with a blue filter which can be used with $CaSO_4$:Tm covered with mica. The most satisfactory dosimeters tested have been made with $CaSO_4$:Tm with protective layers of mica, but the $CaSO_4$:Sm phosphor with a Kapton covering has not been entirely rejected.

3. DESCRIPTION OF FIELD READER

The assembled reader is shown in Fig. 2 with two of the disc-shaped dosimeters in front. This model is approximately 30 cm x 20 cm x 20 cm and weighs about 10 kg. Fig. 3 shows the general mechanical layout and the location of the three removable circuit boards. An expanded view of

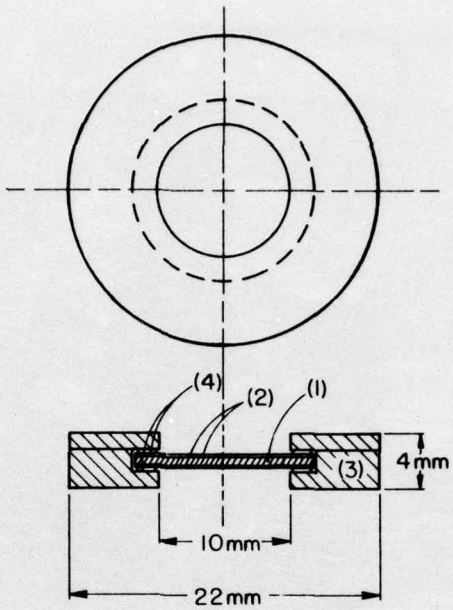

(a)

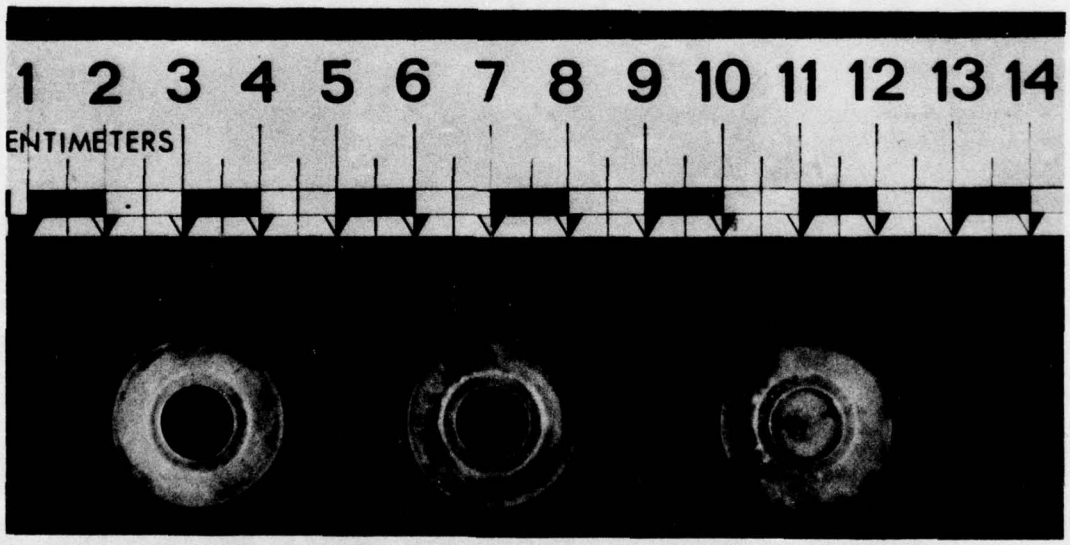

(b)

Fig. 1. Thermoluminescent dosimeters used with the field reader
(a) Details of dosimeter. (1) Polyethylene/phosphor matrix, ten parts cross-linked polyethylene to one part $CaSO_4$:Tm by weight, (2) protective, supporting layer of 25-μm Kapton tape or mica, (3) Plexiglas supporting frame, (4) Kapton washer.
(b) Some experimental dosimeters.

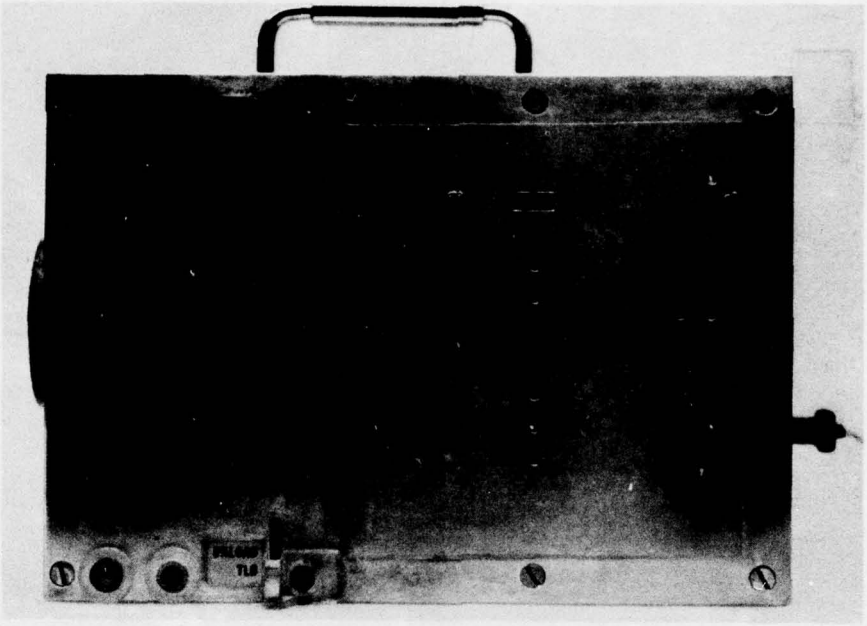

Fig. 2. Experimental model of field reader for combined neutron/gamma thermoluminescent dosimeters. Two of the dosimeters to be used with this reader are shown at left in front of the reader. The instrument is 20 cm in height and the dosimeters are 2.2 cm in diameter.

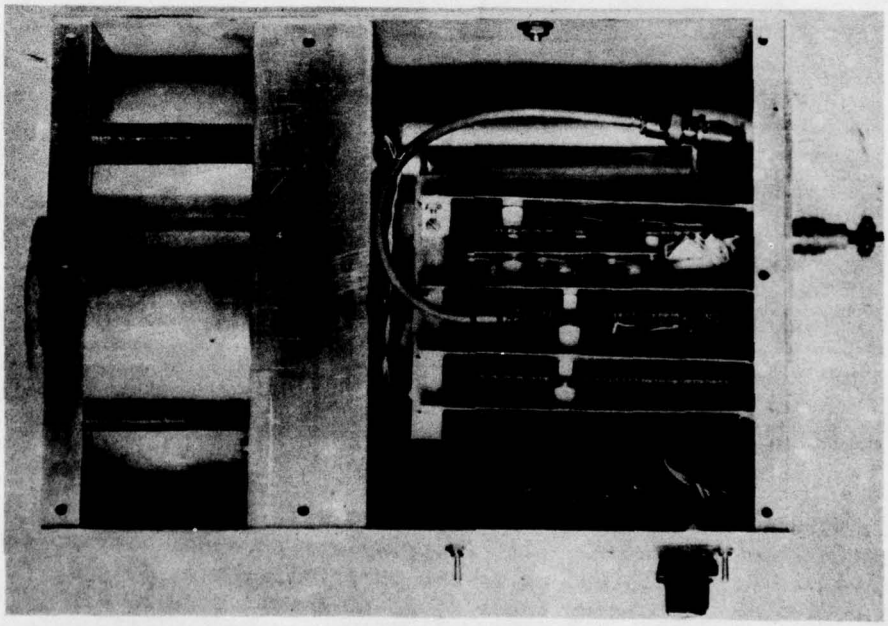

Fig. 3. Reader viewed from above with the top removed.

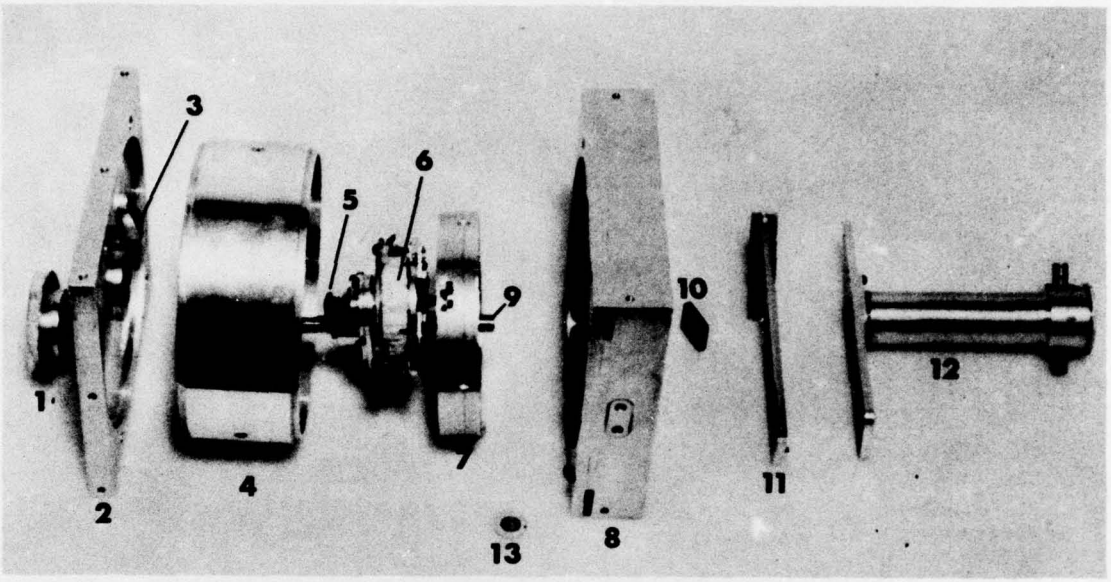

Fig. 4. Exploded view of reader showing principal mechanical parts. (1) knob, (2) back plate, (3) cam, (4) cylindrical shell, (5) cam follower, (6) heater transformer, (7) rotatable cylinder, (8) supporting block with cylindrical surface 100 μm larger in radius than (7), (9) axle, (10) optical filter, (11) filter holder, (12) photomultiplier case, (13) dosimeter.

the various mechanical parts is shown in Fig. 4 with some further details in Fig. 5 and Fig. 6. The three circuit boards contain: (1) the power supplies; (2) the amplifier and integrator circuits for the photomultiplier; (3) the control circuitry, which establishes the READ cycle, and the readout logic.

3.1 Interfacing the Dosimeter with the Reader

One of the prime considerations in the design of the dosimeter and reader is that minimum handling of the dosimeter be required to interface it with the reader. The dosimeter is inserted through the upper slot seen in Fig. 2 and Fig. 3 and through the upper slot in part (8) of Fig. 4. Cylinder (7) mates closely with part (8) and is rotated within (8) by means of knob (1), having three positions (LOAD/CAL, UNLOAD/ZERO, and READ) as indicated opposite the knob and by the LED's (light-emitting diodes) on the front panel. The dosimeter falls into the slot in part (7) (see Fig. 5) when (7) is in the LOAD position. It is then rotated within (7), along with the heater (14) (see Fig. 6) and transformer (6), through 135° to the READ position opposite the photomultiplier tube which is located in (12). As the READ position is approached part (5) rides up cam (3) pushing the heater into contact with the dosimeter. At the same time, cam (15) activates a microswitch inside (4) initiating the READ cycle which includes turning on the heater power. The central, heated portion of the dosimeter, defined by a 3-mm aperture opposite the heater, is viewed through this aperture by the photocathode.

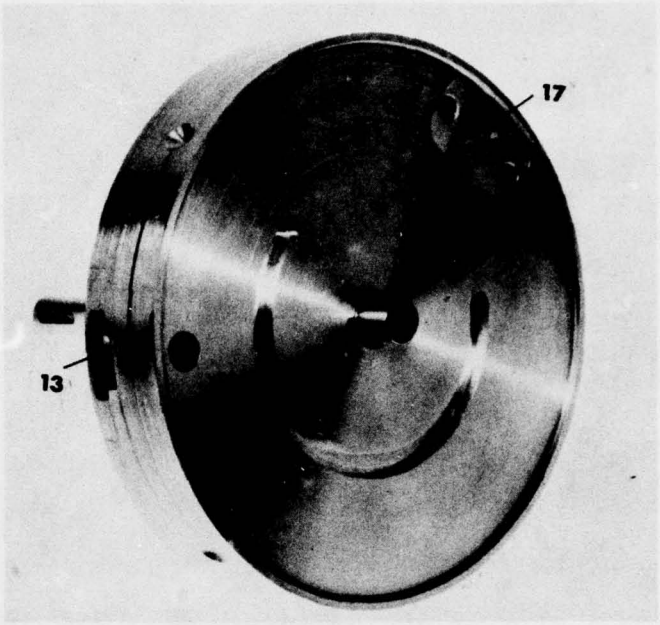

Fig. 5. Rotatable cylinder (part (7) of Fig. 4). (13) Dosimeter, (17) calibration light source.

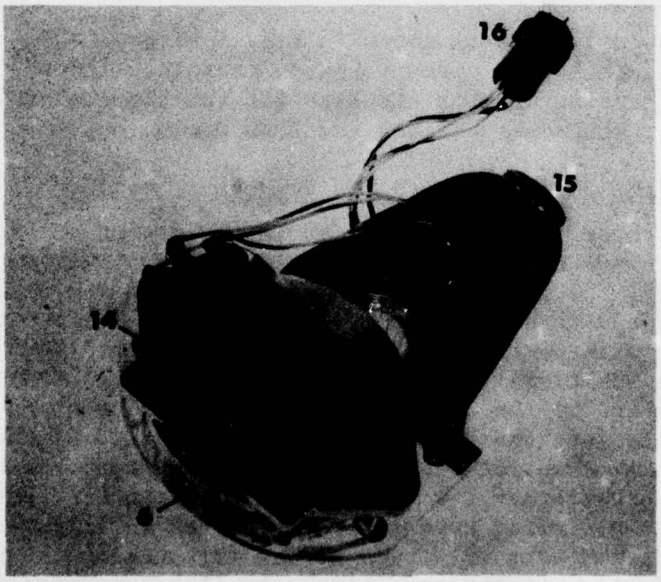

Fig. 6. Heater/transformer assembly. (6) transformer, (14) heater, (15) cam for operation of microswitches inside part (4) of Fig. 4, (16) electrical connector which plugs into connector in part (4).

When the timed READ cycle has terminated, cylinder (7) is rotated back through the LOAD position to the UNLOAD position where the dosimeter is permitted to fall out through the lower slot in the front of the reader case.

The curvature of parts (7) and (8) serve as a light seal to prevent light from the inlet and outlet slots from reaching the photocathode. With a clearance of 100 μm no appreciable light reached the photomultiplier tube even without any treatment of the curved surfaces to reduce reflection.

3.2 The Heating System

One of the most difficult problems in the design of the dosimeter system is that of heating the dosimeter phosphor rapidly and efficiently. The most convenient electrical arrangement would employ a heater which operates directly from the 24-V battery. To obtain an adequate resistance for this voltage requires a length of resistance wire which must be wound on a supporting form which, of course, is also subjected to heat. A number of heaters were wound for operation from 24 V, but problems with electrical insulation and heat transfer to the sample made this heating mode unattractive.

A simple, metal strip heater offers no insulation or fabrication problems and need only be separated from the polyethylene/phosphor matrix by a thin layer of low electrical conductivity. This layer forms part of the dosimeter sandwich mentioned in Sec. 2. So that no additional mass is required to be heated, the metal strip should be self-supporting with sufficient rigidity to make a light pressure contact with the dosimeter. Such metal strips of reasonable length have electrical resistances which are too low for direct operation from 24 V. Consequently, a power converter was required.

The design of an efficient power converter for low-impedance loads led to the adoption of the stainless-steel strip heater (14) shown in Fig. 6. This system is capable of raising the temperature of the heater in contact with the dosimeter 100°C/s. The maximum temperature of the heater (and indirectly that of the dosimeter) is controlled by means of a thermocouple welded to the back of the heater element. The heavy secondary winding made it necessary to rotate the heater transformer along with the heater and the dosimeter. Flexible wires to the transformer primary and to the thermocouple are taken to the connector inside the cylindrical shell (4) of Fig. 4. The power supply for the heater is discussed in some detail in Sec. 3.4.3.

The conduction of heat from the heater through the dosimeter sandwich is treated by computational methods in the Appendix. Comparison of measured light output from the dosimeters (see Sec. 3.3) with calculated emission shows that the heat transfer occurs as expected from the accepted thermal constants for polyethylene with an equivalent thickness of about 0.2 mm of polyethylene added for imperfect thermal contact between the heater and the dosimeter matrix.

3.3 Light Detection and Instrument Calibration

An E.M.I. 9524S photomultiplier tube is used to measure the thermoluminescence emission. This tube was chosen for the detection of $CaSO_4$:Tm emission, having a high efficiency for blue light. Its efficiency for $CaSO_4$:Sm emission in the yellow is about 15% of that for $CaSO_4$:Tm.

The photocathode is positioned about 4 cm from the dosimeter and views the centre portion of the dosimeter matrix through a 3-mm aperture as described above. A light filter (10) in Fig. 4 may be used to reduce background by matching it with the emission of the phosphor to be used. The filter can be changed or removed for cleaning by sliding out the filter holder (11). Leakage of external light to the photocathode was not observed except when the filter holder was slid out from its normal position.

Using a blue filter, a 0.5-mm-thick dosimeter matrix, composed of 10% $CaSO_4$:Tm and 90% cross-linked polyethylene (by weight) in the configuration of Fig. 1, yields a photomultiplier output charge of about 20 nC per rad when the heater is cycled to 300°C for 20 s. By comparison, the dark current is typically 0.7 nA at 20°C within one minute of applying the high voltage (-800 V) to the photomultiplier cathode, resulting in a charge of 140 nC (equivalent to 7 rad) over the 20-s cycle. This dark current is nulled by adjustment of the ZERO-ADJUST knob on the front panel (see Fig. 2) reducing the error due to dark current to less than 1 rad. The null point is achieved when both LED's above this knob are off with the rotatable cylinder in the UNLOAD/ZERO position.

The instrument is calibrated by irradiation of dosimeters to a known dose and by adjustment of the light-detection efficiency and amplification so that the output reading corresponds to this dose. Amplifier gain is varied by means of the CAL-ADJUST knob on the front panel. A calibration light source is provided to compensate for any subsequent changes in amplification, such as a change in photomultiplier gain resulting from a change in supply voltage.

In the LOAD/CAL position the calibration light source is positioned in front of the photocathode. This source consists of a plastic scintillator containing ^{14}C (a low-energy beta emitter) as described by Facey (4). Its emission is predominently blue and, using the same filter as for $CaSO_4$:Tm, produces a photomultiplier current of about 100 nA. With the amplifier gain set by calibration, a voltage level is set equal to the amplified signal from the light source, the balance being indicated by the LED's above the CAL-ADJUST knob. At later times, when the photomultiplier-tube sensitivity or gain may be different, the amplified calibration-light signal can be rebalanced against this preset voltage by adjusting the CAL-ADJUST knob, thus retaining the instrument calibration.

While a record of the thermoluminescence emission is not practicable or necessary in a field reader, this model is provided with terminals from the output of the amplifier following the photomultiplier and from the thermocouple. This facilitates in establishing the heating and timing conditions required for consistent interpretation of the dose to the dosimeters.

Some typical records of the thermoluminescence output from the dosimeters (irradiated by 25 rad of ^{60}Co gammas) are shown in Fig. 7, along with the corresponding heater temperatures. Considerable difference is noted between dosimeters which were read immediately after irradiation and those which were post-annealed at 90°C for 20 min. The initial sharp peak of the unannealed samples is due primarily to emission from low-energy traps. Measurement with a commercial reader of radiation-induced thermoluminescence from powder of the same phosphor heated at 1°C/s show emission peaks at about 50, 100 and 200°C. Because of the high heating rate (100°C/s) of the heater in the reader and because of the lag in heating over the thicknesses of the dosimeter matrices, the emission peaks from the dosimeters overlap extensively. Computer calculations were carried out to interpret the measured light output, such as in Fig. 7, in terms of the energy level of the luminescent traps and the physical properties of the dosimeters. The results are discussed in Appendix at the end of this report.

Thermoluminescence emissions which peak at 50, 100, and 200°C (at 1°C/s heating rate) have half-lives at 20°C of about 2 min, 5 h and 10 y, respectively (see Appendix). Thus, unless the low-temperature traps can be removed, the reading of the dosimeters will be a function of the time which elapses between irradiation and reading. It is known that the low-temperature traps can be reduced in magnitude relative to the 200°C trap by control of phosphor impurity. It is hoped that this offers an effective approach to eliminate the low-temperature peaks. If this approach fails, it may be necessary to empty the low-temperature traps by post-irradiation annealing. Since it is impracticable, in a military operation, to subject the dosimeters to a separate annealing procedure before reading, the annealing should be done during the reading cycle. The heater could be held at an intermediate temperature for a few seconds before light collection begins and before raising the dosimeter to its final readout temperature. This would require a longer readout time and some modifications in the control circuitry.

The intensity curve for the 0.2-mm dosimeter in Fig. 7(a) shows two distinct peaks the first of which is removed by the post-irradiation annealing. It can be seen that this dosimeter can be read in less than 10 s with very little error being introduced because of traps which remain filled. This volume of dosimeter matrix should provide adequate sensitivity according to the discussion at the beginning of this section.

Fig. 7(b) shows that the emission from the 0.4-mm dosimeter has fallen to a few per cent of its maximum at the end of the 20-s heating cycle and consistent readings from this thickness should be obtainable in about 15s. On the other hand, considerable intensity remains at 20 s from the 0.8-mm dosimeter as seen in Fig. 7(c). In fact, calculations in the Appendix of this report show that for thick samples the temperature at the outer edge of the dosimeter matrix can reach an equilibrium value below that required for the 200°C trap to be emptied efficiently. It can be concluded that the reading obtained from the 0.8-mm dosimeter could vary considerably with the maximum heater temperature and inconsistent readings might be obtained.

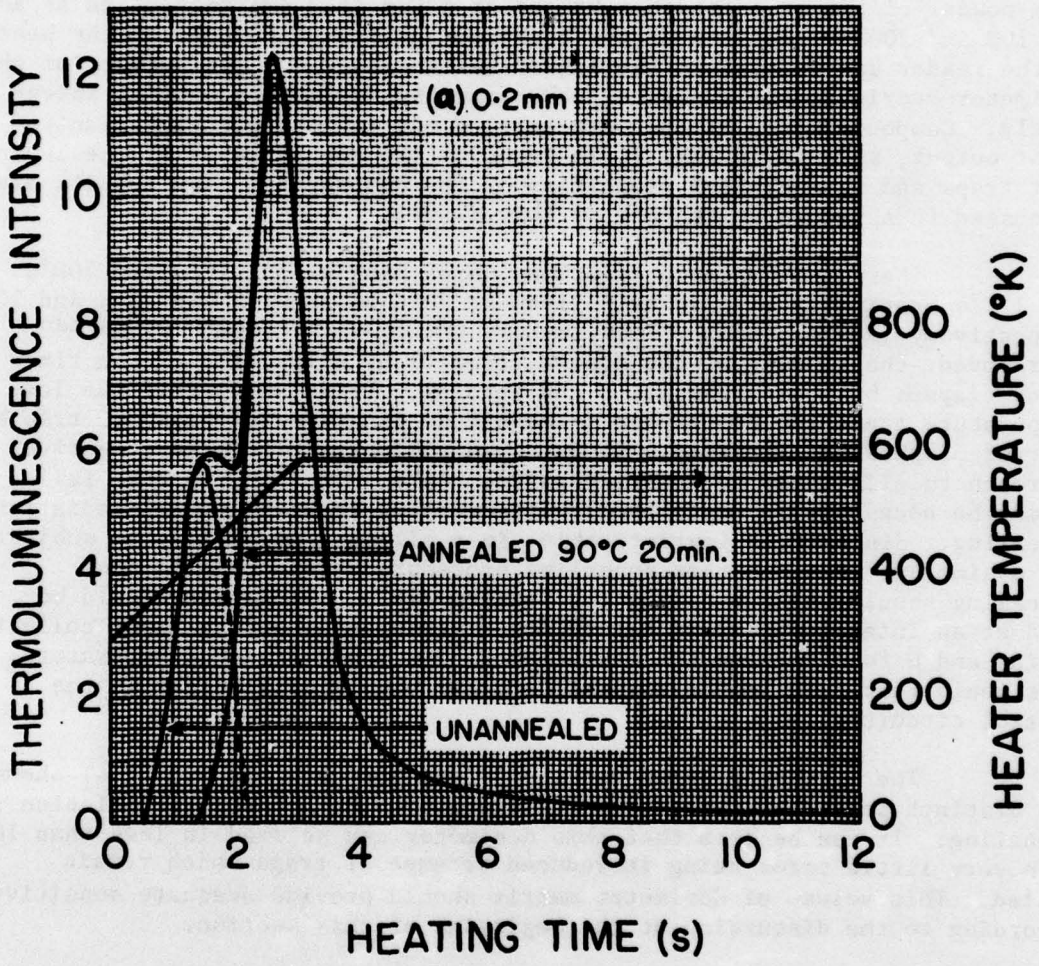

Fig. 7. Thermoluminescence from dosimeters read by the field reader. The intensity is shown for three thicknesses X of the dosimeter matrix with post-irradiation annealing at 90°C for 20 min. and with no annealing. The difference between unannealed and annealed intensity is shown as the dashed curve. (a) X = 0.2 mm.

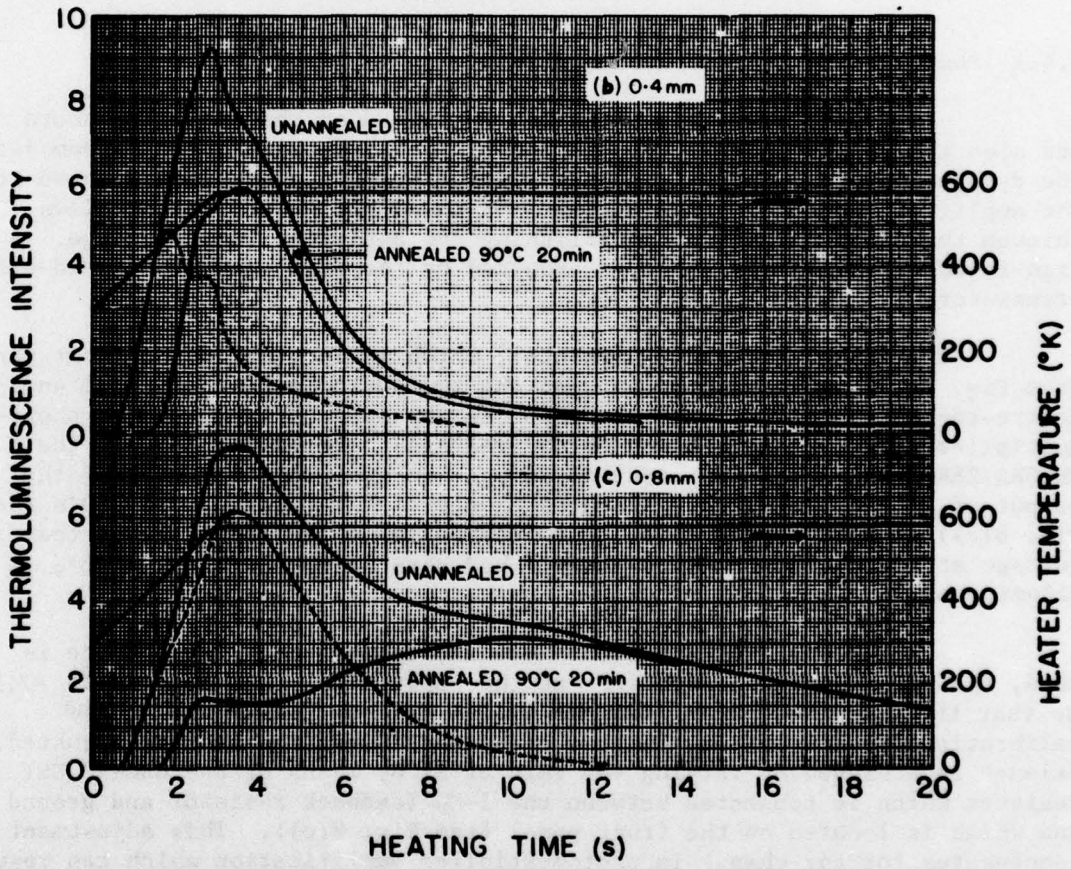

Fig. 7 (continued). (b) X = 0.4 mm, (c) X = 0.8 mm.

Because of the limited number of dosimeters available, the complete dosimeter/reader system has not been checked for linearity, but the phosphors used are known to behave linearly over the dose range of this instrument.

3.4 Electronic Circuitry

The circuit diagrams for the field reader are shown in Fig. 8. 8(a), 8(b) and 8(d) represent the circuits contained on the three circuit boards seen in Fig. 3. In addition, the photomultiplier tube is included in 8(a) and the heater and its transformer are shown in 8(d). Fig. 8(c) represents the LED's and other components mounted on the front panel and also includes the position microswitches and the external battery.

3.4.1 Photomultiplier Tube and Amplifier

Fig. 8(a) shows the circuitry contained on the amplifier board and also the connections to the photomultiplier-tube base which accommodates the dynode resistor chain. The photomultiplier-tube anode is connected to the amplifier input by a coaxial lead and the input anode current flows through the 470-kΩ resistor establishing the amplifier input voltage. A high-impedance amplifier input is provided by the dual, junction field-effect transistor Q1.

The 10-kΩ ZERO-ADJUST resistor, which is located on the front panel (see Fig. 8(c)), is connected between the two source resistors of Q1 and centre-tapped to -7.5 V. This resistor is adjusted to null out the photomultiplier dark current and any offset voltage of amplifier A1. In the UNLOAD/ZERO position, comparator A5 is used to sense the polarity of the output of A1. At imbalance, A5 turns on one or the other of the LED's (see Fig. 8(c)) above the ZERO-ADJUST knob depending on the polarity, so that zero voltage at the output of A1 is established when neither of these LED's is illuminated.

In the LOAD/CAL position where the calibration light source is used, the 100-kΩ variable resistor at the input of A5 is connected to -7.5 V so that the output of A1 is compared with a voltage determined by the calibration procedure (Sec. 3.3), whereby the 100-kΩ resistor is adjusted. Balance is achieved by varying the gain of A1 by means of the CAL-ADJUST resistor which is connected between the 1-MΩ feedback resistor and ground and which is located on the front panel (see Fig. 8(c)). This adjustment compensates for any change in photomultiplier amplification which can result, for example, from a small change in the high-voltage supply.

The signal from the photomultiplier tube is integrated as the output voltage of A1 establishes a current through the 1-MΩ resistor to the input of A2 and builds up a charge on the feedback capacitor C1. C1 is shorted temporarily when the READ cycle is initiated (see Fig. 9 for the sequence of operations during the READ cycle) so that the subsequent voltage at the output of A2 becomes proportional to the integrated light output from the dosimeter. At the end of the READ cycle this voltage is proportional to the dose to the dosimeter.

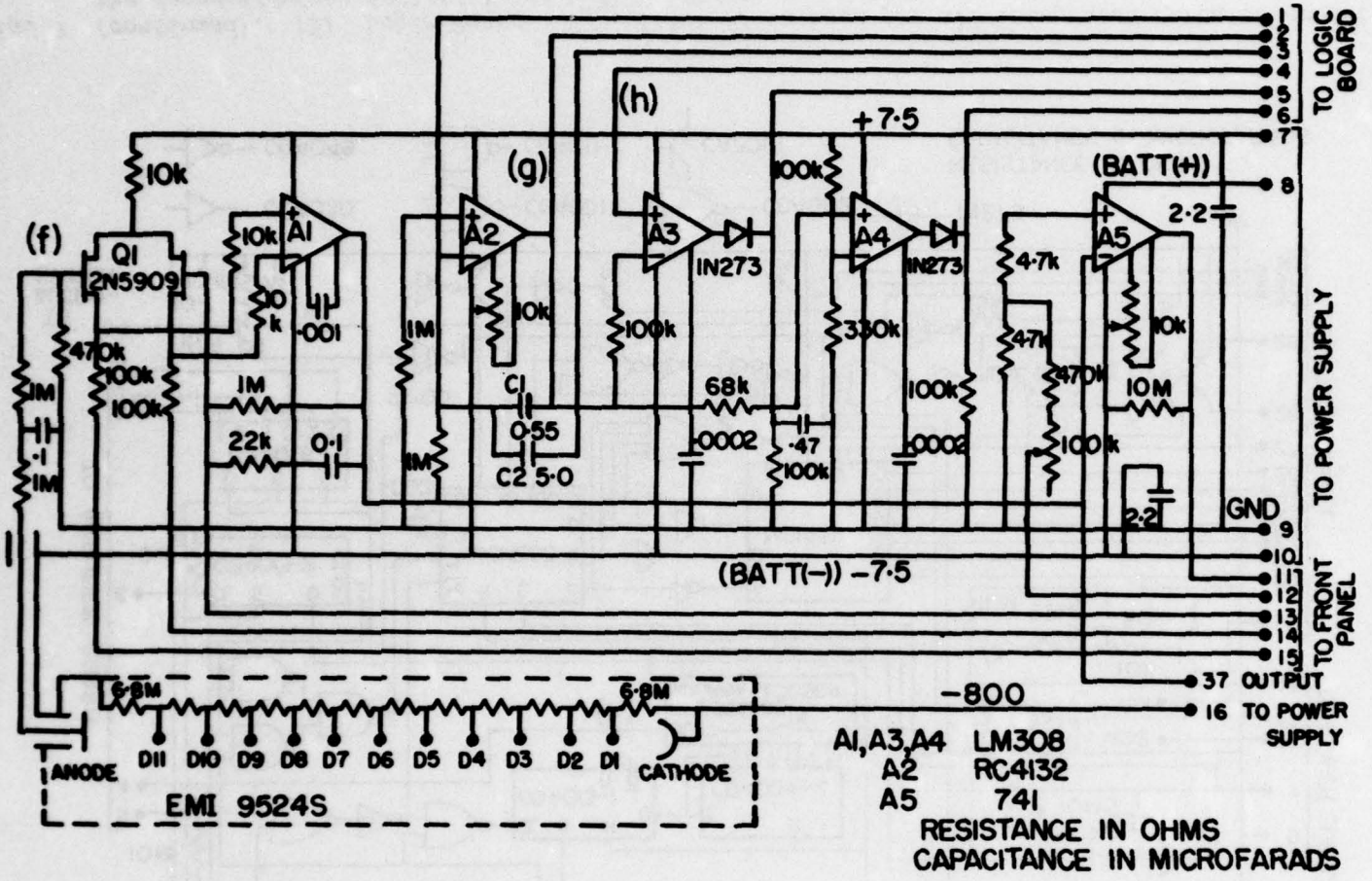

Fig. 8. Circuit diagrams of field reader. Common terminal numbers at the sides of the diagrams 8(a), (b), (c) and (d) indicate connections between circuit boards. (a) Photomultiplier tube and amplifier board.

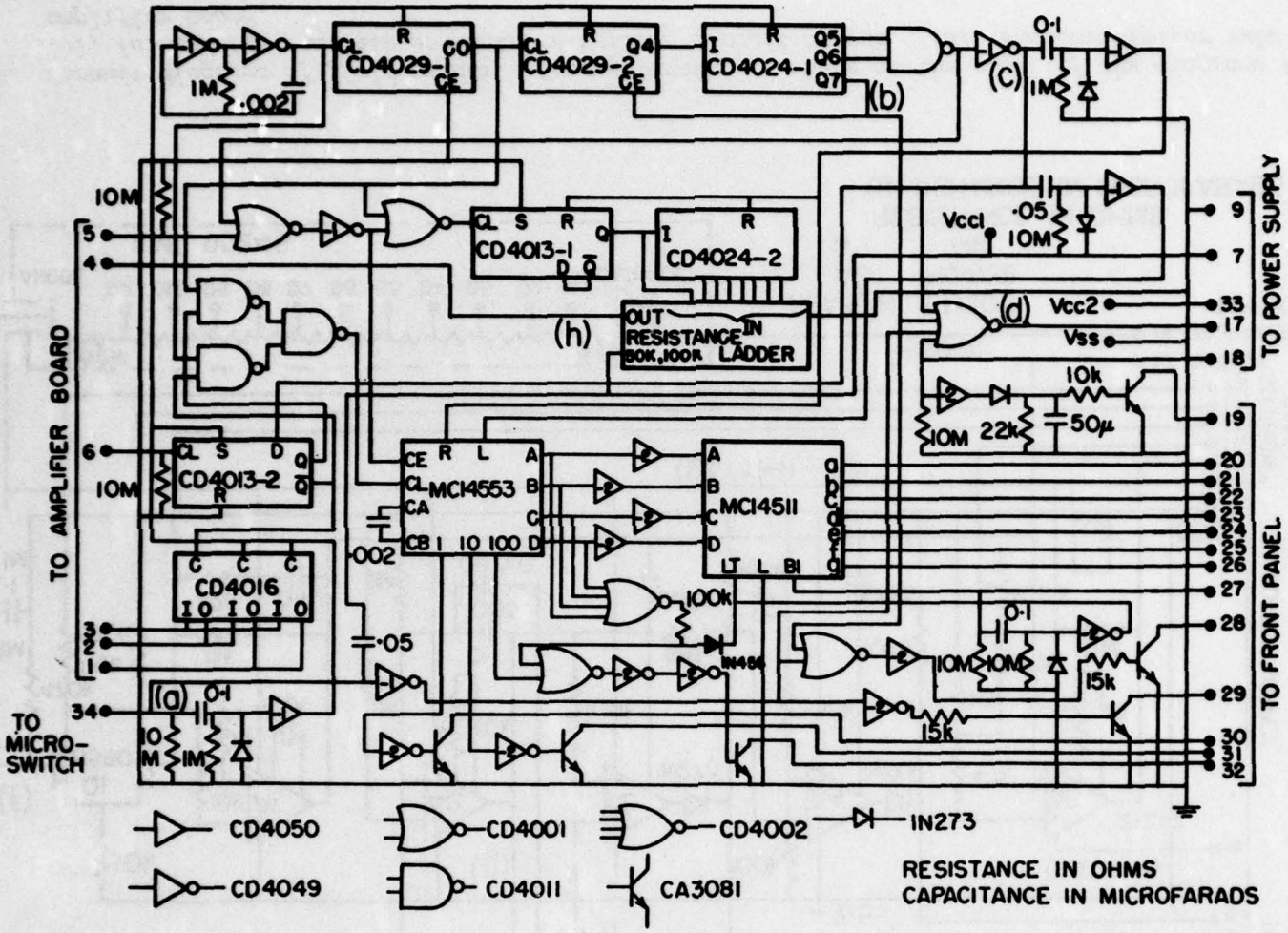

Fig. 8 (continued). (b) Logic Board. V_{cc1} (+7.5 V) is used for all integrated circuits except for the decoder/driver (MC14511) and buffers CD4050-2 and CD4049-2 which use V_{cc2} (+3.6 V).

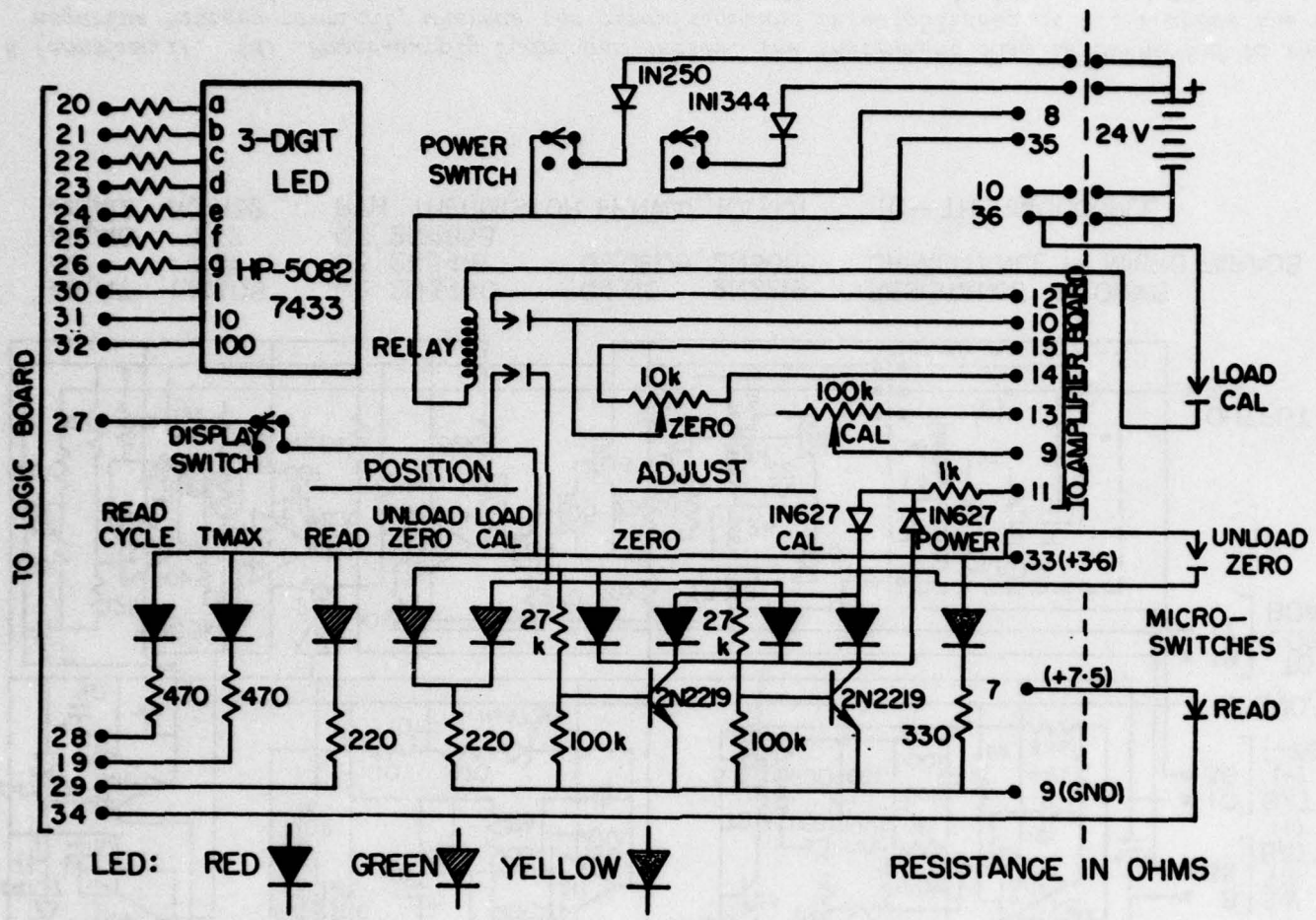

Fig. 8 (continued). (c) Front panel and position microswitches. The 24-V battery is, of course, external.

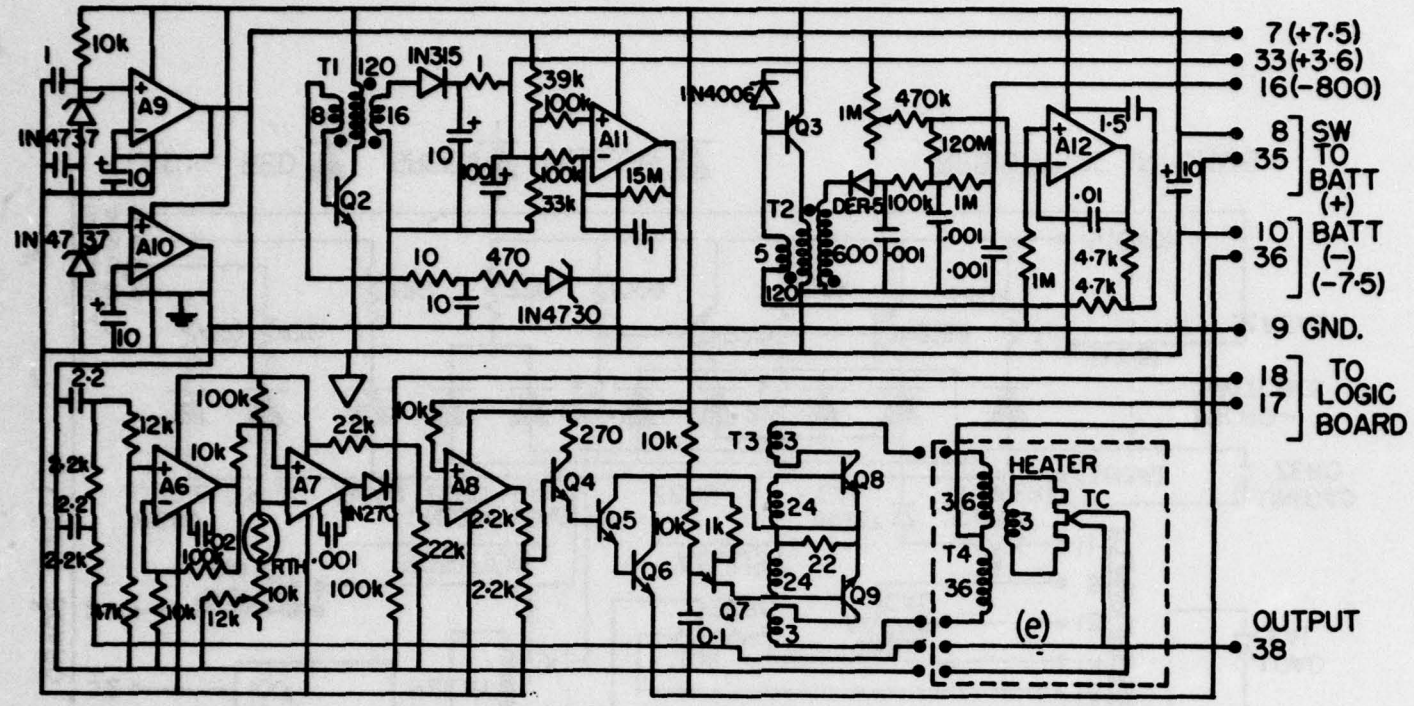

Fig. 8 (continued). (d) Power-supply board and heater. The instrument case is connected to the negative battery terminal, whereas the circuit ground is established at 7.5 V above the negative battery potential. The heater and its transformer T4 are seen in Fig. 4. and Fig. 6.

A3 is used to compare the output of A2 with an internally generated voltage as part of an analog-to-digital converter, while A4 is used for range-switching which includes adding C2 in parallel with C1 when the voltage at the output of A2 exceeds about 5 V.

3.4.2 Control and Readout

The circuits used to control the READ cycle and the readout logic are shown in Fig. 8(b), and the sequence of voltages involved in establishing this cycle are seen in Fig. 9. The letters in Fig. 9 refer to locations in the circuit of Fig. 8(b). Except for the drive transistors of CA3081 and MC14511 all of the circuits in 8(b) are low-power CMOS logic.

The two inverters at the upper left of Fig. 8(b) are used as an oscillator to establish clock pulses. These are fed through two ÷10 counters into the 7-bit binary, program counter CD4024-1 which establishes the states shown as (b) and (c) in Fig. 9. With the oscillator R-C combination shown in 8(b) the clock frequency is approximately 250 Hz giving a total READ-cycle time of about 25 s.

The READ cycle is initiated by rotating the dosimeter to the READ position. As the READ position is approached and the dosimeter contacts the heater, a cam ((15) of Fig. 5) closes a microswitch (the READ microswitch in Fig. 8(c)) which resets the program counter and temporarily shorts the integrating capacitors as mentioned above. Power to the heater is enabled by a high voltage state at (d) of Fig. 8(b) as seen in Fig. 9. This requires the READ microswitch to be closed, the program counter to be in the first three quarters of its cycle and the heater temperature to be below a preset value. The heater temperature is depicted as (e) in Fig. 9. As the dosimeter becomes heated, its luminescence rises to a peak as illustrated by (f) in Fig. 9 and the voltage on the integrating capacitor in 8(a) rises as shown by (g). If this voltage exceeds about 5 V, the output of A4 becomes positive and the instrument switches to a less sensitive range as a result of a clock pulse from A4 to flip-flop CD4013-2. One of the switches of CD4016 is closed for the remainder of the READ cycle paralleling C2 with C1 and resulting in the sudden drop shown in (g). Normally, the input pulses to both the readout counter MC14553 and to the ladder counter CD4024-2 are of frequency f/10, f being the clock frequency. On switching to the less sensitive range the frequency to the readout counter is increased to f while that to the ladder counter remains at f/10.

At the end of the third quarter of the READ cycle the heater is turned off and the readout and ladder counters are reset and then enabled. The resistance-ladder output ((h) in Fig. 9) is directly proportional to the count retained in the ladder counter. When this voltage reaches the output voltage of A2, A3 changes state disabling the ladder and readout counters simultaneously. The counts in the readout counter are, therefore, proportional to the voltage on the integrating capacitor and the dose received by the dosimeter. Calibration consists of adjustment of the amplification of the system so that the readout counts are equal to the dose in rads which would be absorbed in tissue.

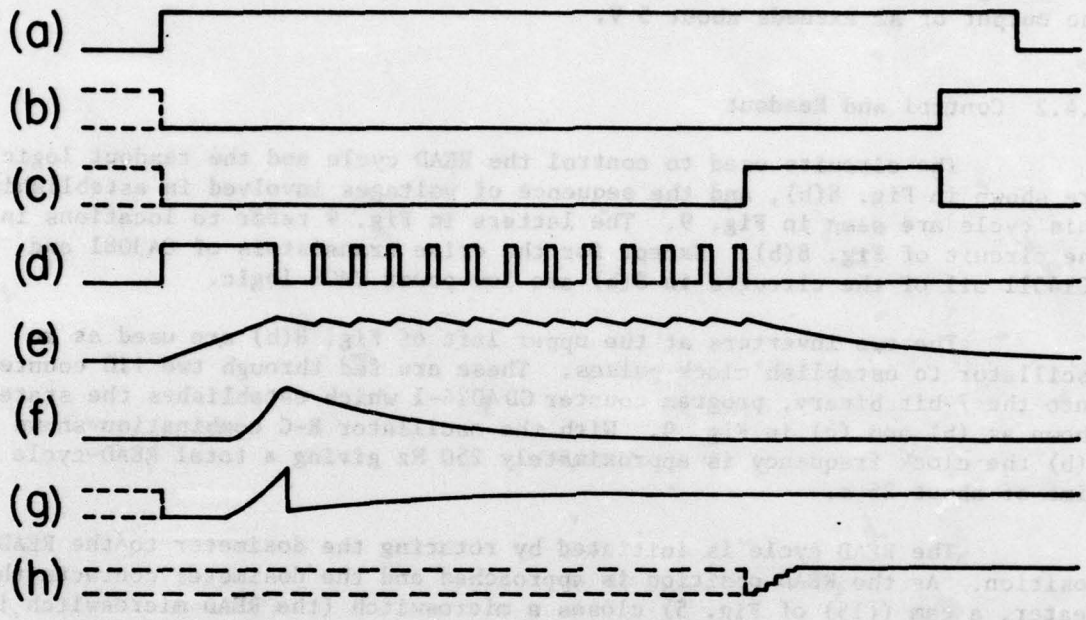

Fig. 9. Voltages of some key circuit locations in the field reader during the READ cycle of a dosimeter. Letters refer to locations identified in Fig. 8(b) and components referred to are those of Fig. 8(b) unless stated otherwise. Dashed lines show uncertain states which depend on preceeding conditions.

(a) READ microswitch. High when rotatable cylinder is in the READ position; rise provides reset pulse for program counters 4029-1, 4029-2 and 4024-1 and also pulse to short integrating capacitors C1 and C2 of Fig. 8(a) via gates 4016.

(b) Last output of program counter. Rise terminates the READ cycle and provides a latch pulse for readout counter 14553.

(c) From program counter. Rise provides reset pulse for ladder (4024-2) and readout (14553) counters; also enables counts from clock to accumulate in these counters.

(d) Power to heater. After initial heating lag in temperature control causes power to come on for short bursts as shown.

(e) Thermocouple potential, closely related to heater temperature above ambient (see Fig. 8(d)).

(f) Photomultiplier-tube output, proportional to rate of thermoluminescence emission from dosimeter (see Fig. 8(a)).

(g) Voltage due to integrated charge (or light output). Drop in voltage corresponds to a range switch with the addition of C2 in parallel with C1 (see Fig. 8(a)).

(h) Ladder output. Counts to ladder are terminated when this voltage reaches that of (g).

The latch pulse at the end of the READ cycle transfers the counts in the readout counter to the counter output for interface with the 3-digit LED display on the front panel. This number is retained on the display until the following READ cycle is completed.

3.4.3 Power Supply

To operate the reader from the 24-V-dc supply available from a military vehicle, voltage converters are required to establish; a) well-regulated supplies of ± several volts for the amplifier and control circuits with current capacities of about 10 mA; b) a low voltage (∿1 V) which is capable of supplying 50 to 100 W to the heater; c) approximately 3 V at up to 150 mA for the LED's; d) a regulated high voltage (∿ 800 V) providing a few μA for the photomultiplier tube,

The low-voltage heater supply uses a push-pull oscillator in which either Q7 or Q8 is turned on. These are silicon power transistors capable of switching up to 15 A. The oscillator transformer T3 is wound on a 3-cm-diameter, toroidal, tape-wound core. With the turns indicated in Fig. 8(d) this oscillator produces a square wave at a frequency of 2.5 kHz. Output transformer T4 is the 6-cm-diameter coil mounted directly behind the heater as seen in Fig. 4 and Fig. 6. T4 matches the output from Q7 and Q8 to the low-impedance heater with a step-down ratio of 12:1. A current of approximately ±70 A is delivered to the 0.015-Ω heater for a power output of about 70 W. Disregarding heat losses, about 80 J are required to heat the heater strip to 300°C and about 30 J are required to heat 50 mm^3 of polyethylene corresponding to the dosimeter. In practice, the heater temperature reaches 300°C in about 3 s.

The heater supply is controlled by switching Q6 to permit or deny current to the oscillator. Unijunction transistor Q9 ensures the initiation of oscillation when Q6 is turned on. The state of Q6 depends on the input to A8 which along with Q4 and Q5 acts as a current amplifier to drive A6. During the heating cycle (determined as outlined in Sec. 3.4.2), the heater power is on provided that the amplified thermocouple voltage (on the (+) input of A7) is exceeded by the reference voltage (on the (-) input of A7) established from the +7.5-V supply. This reference voltage thus determines the maximum heater temperature T_M which can be varied by adjustment of the 10-kΩ resistor. Once T_M is reached, the heater power is on for short bursts, as illustrated in Fig. 9 ((d) and (e)), and the heater temperature goes up and down by about 5°C. Thermistor RTH compensates for changes in ambient temperature making T_M nearly independent of the reader temperature.

The LED power-supply converter uses the blocking oscillator composed of transformer T1 and transistor Q2. A voltage of approximately +3.6 V above circuit ground is established and regulated by reference from the +7.5 V. Overvoltage is amplified by A11 and fed back out of phase to the oscillator.

A similar converter, using T2 and Q3 for the oscillator, is employed for the high-voltage supply. A balance point between the high voltage (nominally -800 V) and the +7.5 V is compared to circuit ground by A12, the output of which is fed back to Q3.

Operating from a 24-V battery, the reader is found to have a power requirement of less than 1 W when the heater is off. With the heater on, approximately 120 W are being taken from the battery. The heater is on about an average of 4 s during a READ cycle for an energy consumption of approximately 500 J per dosimeter.

4. SUMMARY AND CONCLUSIONS

An experimental model of a field reader for a combined neutron/gamma thermoluminescent dosimeter has been designed and constructed. Successful operation of the reader has been demonstrated with a limited number of dosimeters.

The dosimeter/reader system has been found to have a sensitivity such that reading errors due to dark current or extraneous light are less than about 1 rad. The reading accuracy is about ±5% ±1 rad so that the accuracy of the system will probably be limited by the consistency with which the dosimeters can be made.

The system has been designed so that the dosimeter can be quickly inserted into the reader. The present READ cycle of 25 s can be reduced so that up to four dosimeters could be read in one minute.

About 500 J are required to read each dosimeter. At four dosimeters per minute, this would be an average current of 1.4 A from a 24-V battery.

5. RECOMMENDATIONS

To determine that adequate fast-neutron (relative to gamma) sensitivity can be obtained, further research is required into the fast-neutron response of various mixtures of thermoluminescent phosphors and hydrogenous media.

Further effort is required to develop efficient techniques of making the dosimeters for this system in large numbers. This should be followed by extensive tests of the dosimeter/reader system.

6. ACKNOWLEDGEMENTS

The author wishes to thank Mr. R.A. Facey for his many helpful discussions throughout the development of this instrument. Mr. Facey is responsible for the development of the combined neutron/gamma dosimeter matrix. I also wish to thank Mr. L.E. Corish for assistance with details of the mechanical design, Mr. L.P. Rushton for his work on the design and construction of the power supplies, Mr. A. Hollingsworth for his proficiency in the machining of the reader and Mr. R.A. Gravelle who fabricated the dosimeters used with the reader.

7. REFERENCES

1. F.G. Allen, Tactical Dosimeter DT60A/PD and Computer-Indicator CP95A/PD, Engineering Report DGEL-R2, Dept. of National Defence. Canada (1966).

2. United States Department of Defense, "Effects of Nuclear Weapons", Ed. S. Glasstone, United States Atomic Energy Commission, 1964.

3. R.A. Facey and R.A. Gravelle, A Plastic T.L. Dosimeter for Fast Neutrons Plus Gamma Rays. DREO Memo 15/74 (NBC), Health Phys. 27, 621, (1974).

4. R.A. Facey, A Substandard Light Source of Very Low Intensity, J. Sci. Instr. 43, 658. (1966).

PRECEDING PAGE BLANK-NOT FILMED

APPENDIX

A1. Thermoluminescence

Phosphorescent materials are characterized by metastable states which on de-excitation result in luminous emission or luminescence. These states or "traps" can be energized by several means including chemical, mechanical or electrical stimulation. A certain energy or trap depth is required to de-excite the phosphor and this may be derived from optical or thermal sources, for example. We are here concerned with radiation-sensitive thermoluminescent phosphors in which energy from ionizing radiation is absorbed and in which heating results in part of this energy being released in the form of visible luminescence. For a comprehensive treatment of thermoluminescence the reader is referred to Curie (A1) and to Cameron, Suntharalingam and Kenney (A2).

Thermoluminescence emission is expressed by the Randall-Wilkins relation in which the intensity of emission I is given by

$$I = \frac{dn}{dt} = - ne^{-E/kT} \qquad \text{(A1)}$$

where n is the number of filled traps at time t, E is the activation energy or trap depth required to release the trapped particle, T is the absolute temperature, k is Boltzmann's constant and S is a constant generally assumed to be independent of T. Eq.(A1) determines both the length of time an excited phoshpor can be stored without appreciable de-excitation, and the time required to measure the bulk of the emission from a phosphor at an elevated temperature.

At constant temperature, as for storage or annealing, the half-life $t_{\frac{1}{2}}$ of the phosphor according to eq.(A1) is given by

$$t_{\frac{1}{2}} = 0.693/(Se^{-u}), \qquad \text{(A2)}$$

where $u = E/kT$. $t_{\frac{1}{2}}$ is plotted as a function of E in Fig. A1 for $S = 10^9\ s^{-1}$ at the temperature indicated. Since $t_{\frac{1}{2}}$ is inversely proportional to S, $t_{\frac{1}{2}}$ for values of S other than $10^9\ s^{-1}$ are found by multiplying $t_{\frac{1}{2}}$ from Fig. (A1) by $10^9/S$.

In thermoluminescence measurements it is customary to apply linear heating rates to the samples and to observe the emission as a function of

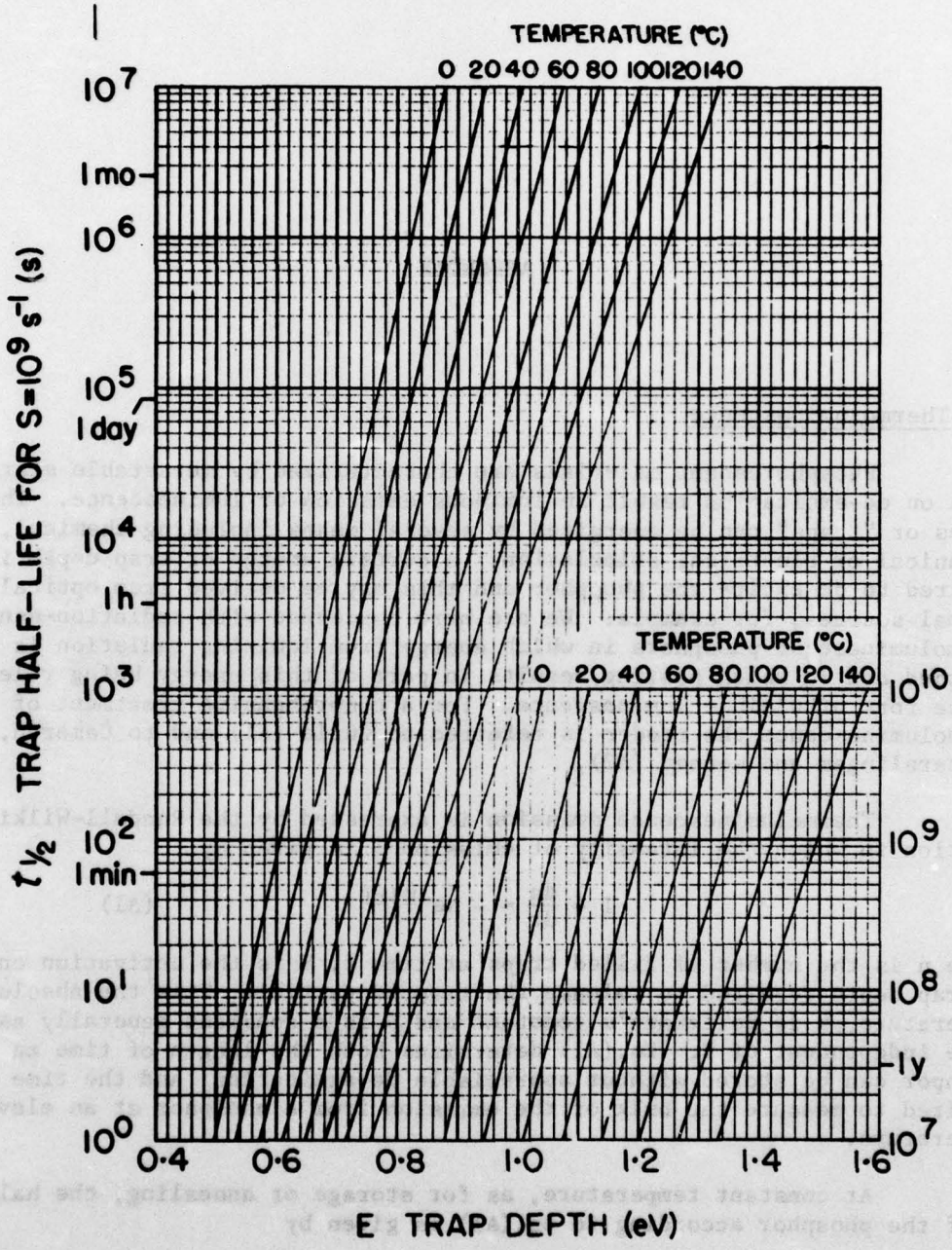

Fig. A1. Half-life for thermal de-excitation of thermoluminescent traps at constant temperature as a function of trap depth, according to eq. (A2) with $S = 10^9\ s^{-1}$.

temperature. With linear heating rate β, eq. (A1) can be written

$$\frac{dn}{dT} = -\frac{nS}{\beta} e^{-E/kT} \qquad \text{(A3)}$$

with the solution

$$n = n_o \exp\left[\frac{ES}{K\beta}\int_{u_o}^{u} \frac{e^{-u}}{u^2}\, du\right] \qquad \text{(A4)}$$

where $u = E/kT = E/k(T_o + \beta t)$. The subscript ● refers to initial conditions before heating. Equating d^2n/dT^2 to zero, shows that maximum emission occurs at the temperature T* for which

$$\frac{e^{-U}}{U^2} = \frac{\beta k}{SE} \quad , \qquad \text{(A5)}$$

U being equal to E/kT*. T* is plotted against E in Fig. A2 for various values of S/β. As seen from eq. (A5), E and S are not determined independently from T* measured at a single β. Furthermore, combinations of E and S, with S ranging over several decades, can be chosen to closely agree with measured T* at values of β also ranging over several decades. As will be shown for specific predictions of dosimeter readings, it is not critical what combination of S and E are used to satisfy a known T*.

However, eq. (A2) and eq. (A5) can be used to eliminate S giving an equation of the form

$$ye^{-y} = C, \qquad \text{(A6)}$$

where $y = \left(\frac{1}{T} - \frac{1}{T^*}\right)\frac{E}{k}$ and $C = \frac{0.693(T^*)^2}{t_{\frac{1}{2}}T}\left(\frac{1}{T} - \frac{1}{T^*}\right)$. As above, the half-life $t_{\frac{1}{2}}$ is measured at constant temperature T, and T* is the temperature for maximum emission at constant heating rate. Solving eq. (A6) for y (we are here interested in solutions for y greater than unity) yields a value of E which, along with eq. (A2), also gives S. This suggests a simple experimental method of determining E and S.

In addition to the occurance of more than one trap depth, each trap depth E represents a distribution of traps about E which complicates the relationships between theory and experiment. For the present calculations discrete levels of E are assumed.

A2. Calculation of Thermoluminescence from Dosimeters in Field Reader

The rate at which the dosimeters can be read in the field reader is limited by the power of the heater system and the rate of transfer of heat to the phosphor. As indicated in Sec. 3.4.3, there is sufficient power available to heat the heater and the dosimeter to the required temperature in a few seconds. Since reading times considerably longer than this are required, the limiting factor appears to be the rate of heat transfer across the dosimeter.

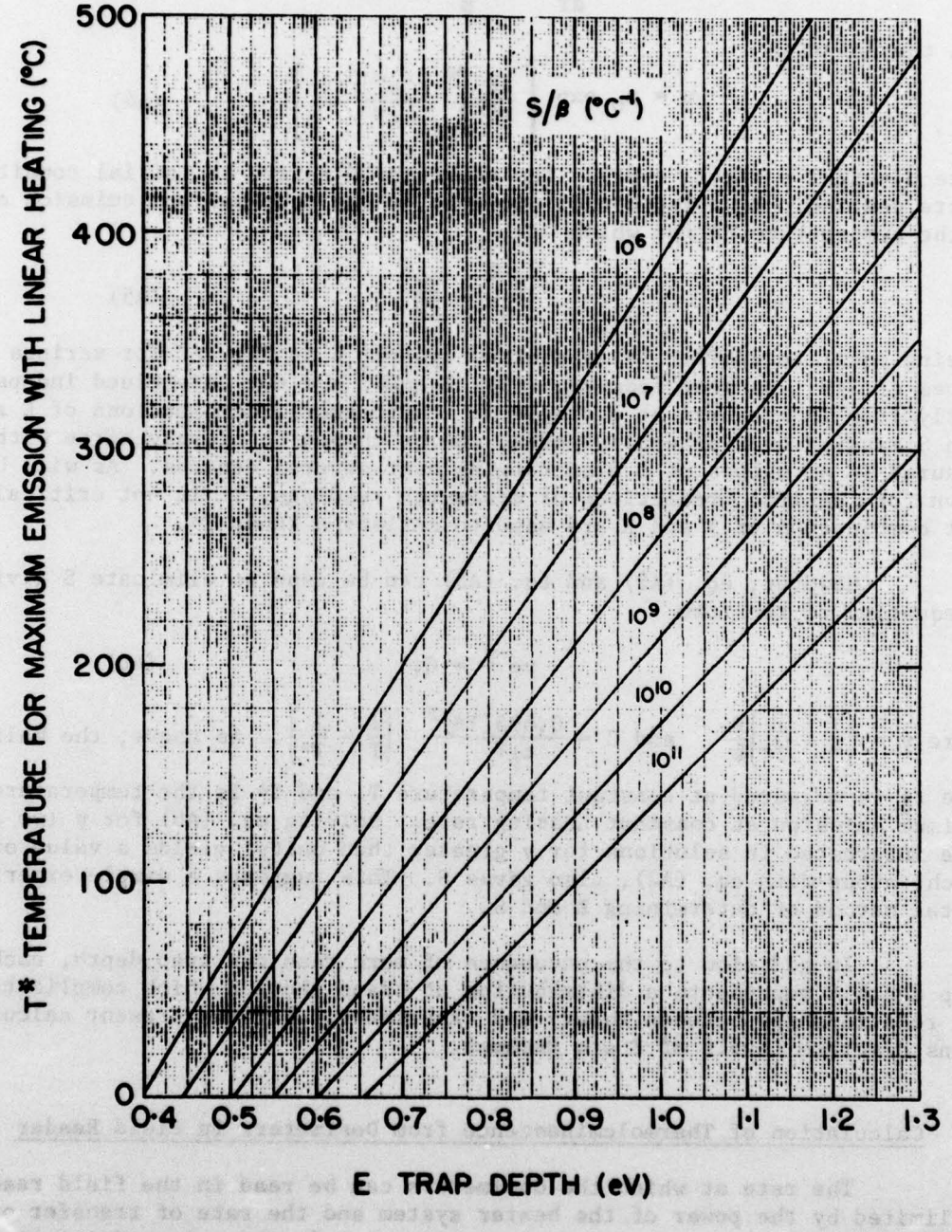

Fig. A2. Temperature for maximum thermoluminescence intensity with linear heating as a function of trap depth, according to eq. (A5) for values of S/β from 10^6 to 10^{11} °C^{-1}.

In treating the thermoluminescence emission from the dosimeter discussed in this report, we are concerned only with the central portion of the dosimeter sandwich adjacent to the heater since only this portion is viewed by the photocathode. The transfer of heat into this volume can be approximated as one-dimensional flow with surface and lateral losses represented by a thermal mass beyond the dosimeter. The dosimeter model for which calculations are made in this appendix is shown in Fig. A3. The layer between the heater and the dosimeter represents imperfect thermal contact in addition to the protective layer over the dosimeter matrix. The heat sink is a convenient means of terminating the calculations. A thermal barrier has also been used for this purpose for some calculations, but the heat sink has been shown to be more appropriate to experimental conditions.

The one-dimensional heat transfer equation is given by

$$\frac{\partial T}{\partial t} = \frac{K}{c\rho} \frac{\partial^2 T}{\partial x^2}, \qquad \text{(A7)}$$

where K is the thermal conductivity, c the heat capacity, ρ the density and t and x are the time and space co-ordinates. Using j and i as time and space indices, eq. (A7) can be approximated as

$$T_{i,j+1} = T_{i,j} + B(T_{i-1,j} - 2T_{i,j} + T_{i+1,j}) \qquad \text{(A8)}$$

where $B = (K\Delta t)/(c\rho(\Delta x)^2)$ and is uniform over the three space intervals.

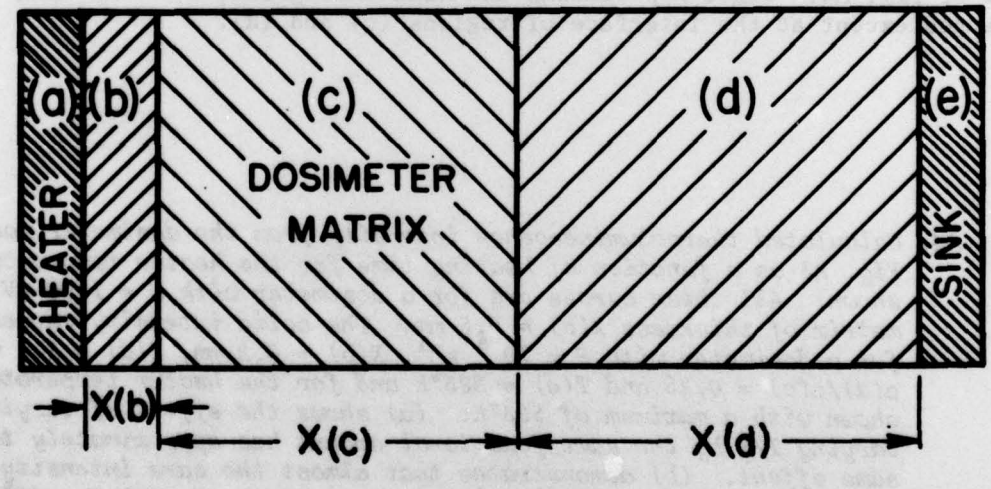

Fig. A3. One-dimensional dosimeter model used for purposes of calculations to represent dosimeter used with field reader. Region (a) heater, (b) insulation between heater and dosimeter matrix, (c) dosimeter matrix, (d) layer used to simulate surface and lateral heat losses, (e) heat sink or thermal barrier used to terminate calculations.

The temperatures of regions (a) and (e) of Fig. A3 are the boundary conditions for eq. (A8). For region (a), the heater, T is taken as rising linearly from ambient temperature to the maximum temperature T_M in 3 s, after which $T = T_M$ during the remainder of the heating cycle. For region (e) T is usually assumed to remain at ambient temperature. Eq. (A8) calculates the temperature for spatial intervals at any time interval using the spatial distribution of temperature from the immediately preceeding time interval.

Temperatures from eq. (A8) are used in eq. (A1) to calculate the emission intensity I as a function of time and position within the dosimeter. Summing I over the dosimeter thickness gives the total emission as a function of time, which can be compared with that measured experimentally.

Results of calculations for a 0.5-mm dosimeter with a trap depth of 1.00 eV are shown in Fig. A4 where the relative thermoluminescence intensity is plotted as a function of heating time for various heater temperatures. The effects of varying one of the other parameters are demonstrated by comparing calculated intensities with that for the dosimeter represented by the solid line, which is typical of the intensity from the dosimeters measured in the field reader. This (solid-line) intensity curve is the result of calculations for a dosimeter for which $S = 10^9\ s^{-1}$, region (b) (of Fig. A3) is 0.2 mm in thickness, region (d) is 1.0 mm in thickness, region (e) is kept at ambient temperature (taken to be 20°C), and $T_M = 593°K$ (320°C). The constants of eq. (A7) were taken to be those for polyethylene ($K = 9\times10^{-4}$ cal $cm^{-1}s^{-1}°C^{-1}$, $c = 0.55$ cal $g^{-1}°C^{-1}$ and $\rho = 0.91$ g cm^{-3}) in regions (b) and (c). For region (d) a lower density and proportionately lower thermal conductivity were used with $\rho(d)/\rho(c) = 0.25$ for the solid-line intensity curve of Fig. A4. Since K/ρ remains the same throughout, B of eq. (A8) is unchanged except at the interface of regions (c) and (d).

Fig. A4. Calculated thermoluminescence intensity from the dosimeter model of Fig. A3 as a function of heating time for the heater temperature shown. All these curves are for a dosimeter with E = 1.00 eV and a matrix of thickness X(c) = 0.5 mm. The solid intensity curves are for a dosimeter with $S = 10^9\ s^{-1}$, X(b) = 0.2 mm, X(d) = 1.0 mm, $\rho(d)/\rho(c) = 0.25$ and T(e) = 293°K and for the heater temperature shown with a maximum of 593°K. (a) shows the effect of varying Tm; varying 1/E by the same fractional amount has approximately the same effect. (b) demonstrates that almost the same intensity curve is obtained with $S = 10^{11}\ s^{-1}$ and E = 1.21 eV as with $S = 10^9\ s^{-1}$ and E = 1.00 eV. The effect of increased temperature losses with $\rho(d)/\rho(c)$ increased to 0.5 is also shown. (c) shows that the effect of increasing X(d) to 2 mm and of replacing the heat sink with a thermal barrier are minimal. Reducing X(d) to 0.5 mm reduces the intensity maximum by decreasing the temperature rise of the dosimeter matrix.

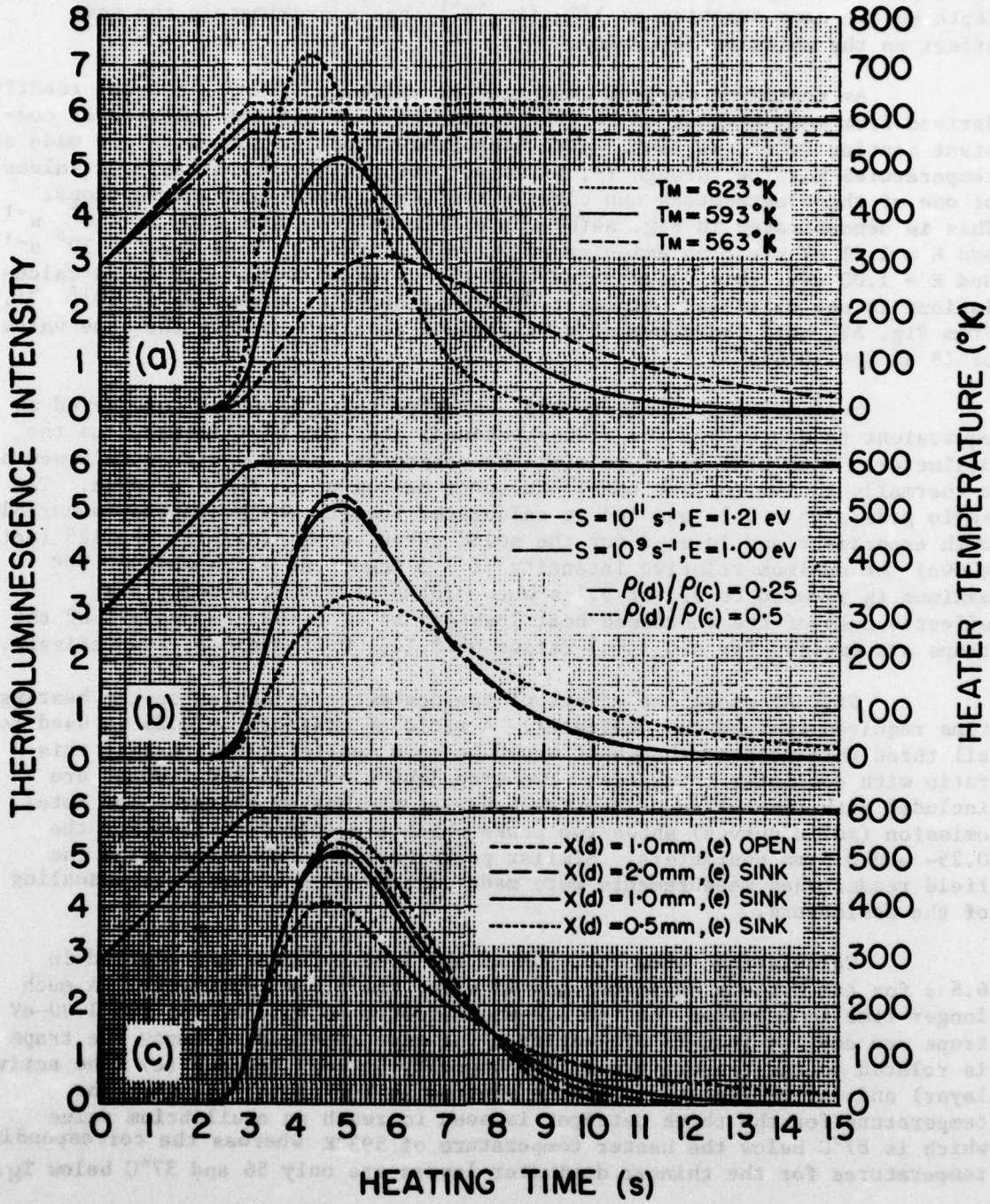

Fig. A4 (continued).

In Fig. A4(a) the dosimeter is heated to 270, 300 or 330°C above an ambient temperature of 20°C (293°K) with the heater temperatures as shown. These intensity curves show considerable shift in the times of emission with 10% changes in temperature elevation. At 10 s, 50, 85 and 99% of the traps are emptied for T_M = 563, 593 and 623°K, respectively. Changing the trap depth by the same fraction as $1/T_M$ (in $°K^{-1}$) has approximately the same effect on the emission intensity.

As mentioned earlier, independent values of S and E are not readily derived from measurements of T* (the temperature of maximum emission at constant heating rate), so that, where measurements of the intensity are made at temperatures passing through T*, it is not surprising that a range of values of one of these parameters can closely represent experimental conditions. This is demonstrated in Fig. A4(b) where calculations made with $S = 10^9$ s^{-1} and E = 1.21 eV yield an emission curve very similar to that for $S = 10^9$ s^{-1} and E = 1.00 eV. This illustrates that the value of S used for these calculations is not critical; at least within an order of magnitude of 10^{10} s^{-1}. From Fig. A2, both the above sets of S and E are seen to have the same value of T* at $\beta = 10°C\ s^{-1}$.

Decreasing the density $\rho(d)$ relative to $\rho(c)$ can be considered as equivalent to decreasing the cross-sectional area for heat losses from the dosimeter. With $\rho(d)$ equal to $\rho(c)$ the dosimeter matrix would be followed by a thermally-equivalent but non-luminescent medium up to the heat sink. The ratio $\rho(d)/\rho(c) = 0.25$ has led to calculated results which compare favourably with experiment and is used for the solid curve. With $\rho(d)/\rho(c) = 0.125$ (not shown) the maximum relative intensity of 7.3 occurs at 4.5 s whereas the maximum is reduced to 3.3 at 5.1 s when $\rho(d)/\rho(c) = 0.5$, showing the effectiveness of the increased heat losses. At 10 s, 92, 85 and 39% of the traps are emptied for $\rho(d)/\rho(c)$ ratios of 0.125, 0.25 and 0.5, respectively.

Fig. A5 shows the effect of the dosimeter thickness on the heating time required to read the dosimeter. A ratio of $\rho(d)/\rho(c) = 0.25$ is used for all three thicknesses, though it would be more realistic to increase this ratio with dosimeter thickness. Two trap depths of 0.75 and 1.00 eV are included with two-thirds of the traps having the higher energy. The total emission (solid curves) shows two peaks which are well separated for the 0.25- and 0.5-mm dosimeters. Similar peaks have been observed using the field reader when measurements were made with no post-irradiation annealing of the dosimeters.

Calculations show that 90% of the 1.00-eV traps are emptied in 6.6 s for the 0.25-mm dosimeter and 11 s for the 0.5-mm dosimeter. A much longer time is required for the 1.0-mm dosimeter as only 67% of the 1.00-eV traps are emptied in 20 s of heating. The time required to empty the traps is related to the temperature at the boundary between regions (c) (the active layer) and (d) of Fig. A3. This is plotted as T(c/d) in Fig. A5. The temperature for the thick detector is seen to reach an equilibrium value which is 87°C below the heater temperature of 593°K whereas the corresponding temperatures for the thinner dosimeter layers are only 56 and 37°C below T_M.

The thermoluminescence-intensity curves of Fig. A5 are similar to measured outputs from dosimeters used in the field reader, such as those of

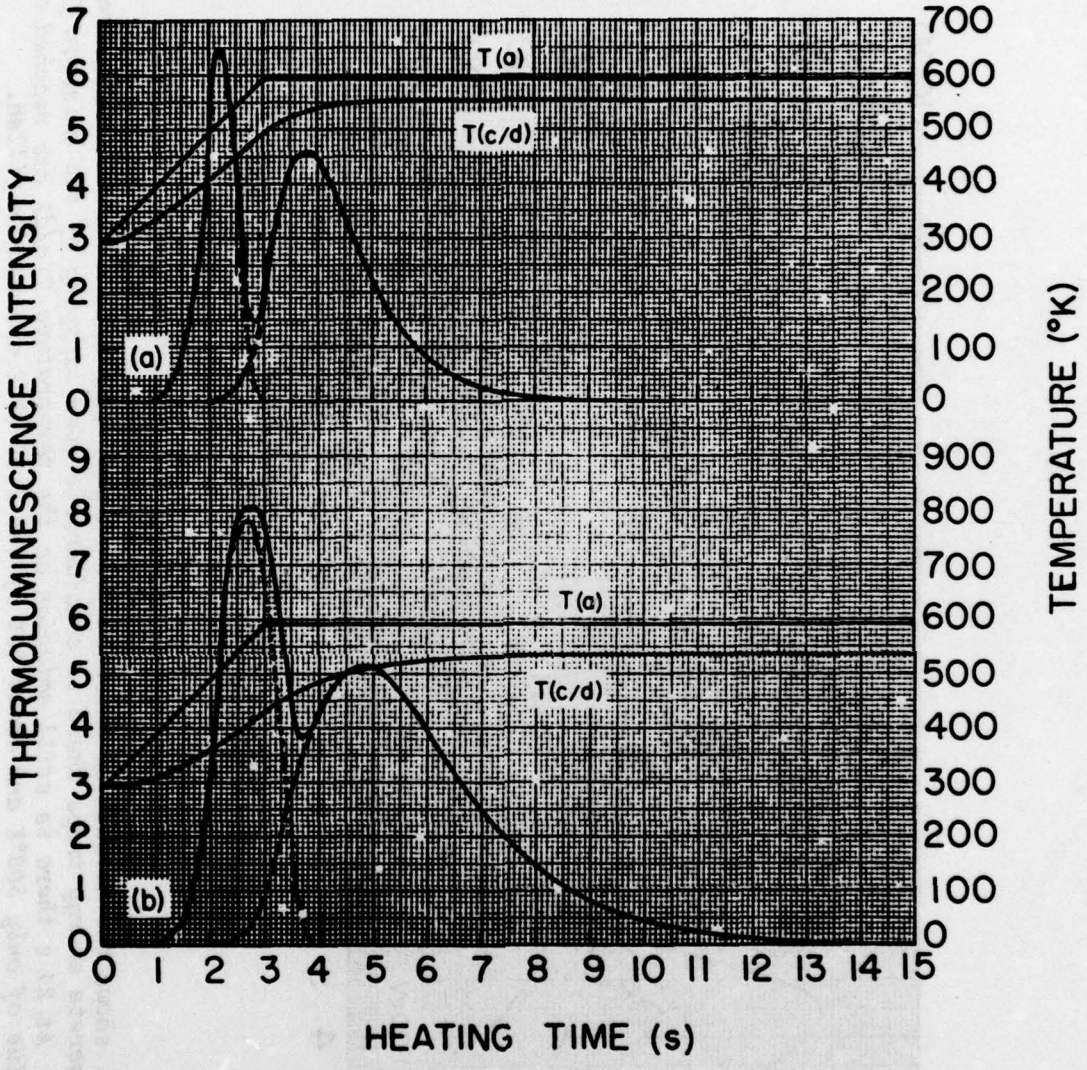

Fig. A5. Calculated thermoluminescence intensity as a function of heating time for T_M = 593°K. The heater temperature T(a) and the temperature T(c/d) at the interface of regions (c) and (d) are also shown. The intensities are for dosimeters having $S = 10^9$ s^{-1}, X(b) = 0.2 mm, X(d) = 1.0 mm, ρ(d)/ρ(c) = 0.25 and T(e) = 293°K. Two temperature traps of energies 0.75 and 1.00 eV are assumed with two-thirds of the loaded traps having the higher energy. The solid curve is the combined emission from all traps. (a) and (b) are for dosimeters with X(c) = 0.25 and 0.5 mm respectively. Emission from the two trap levels are clearly resolved.

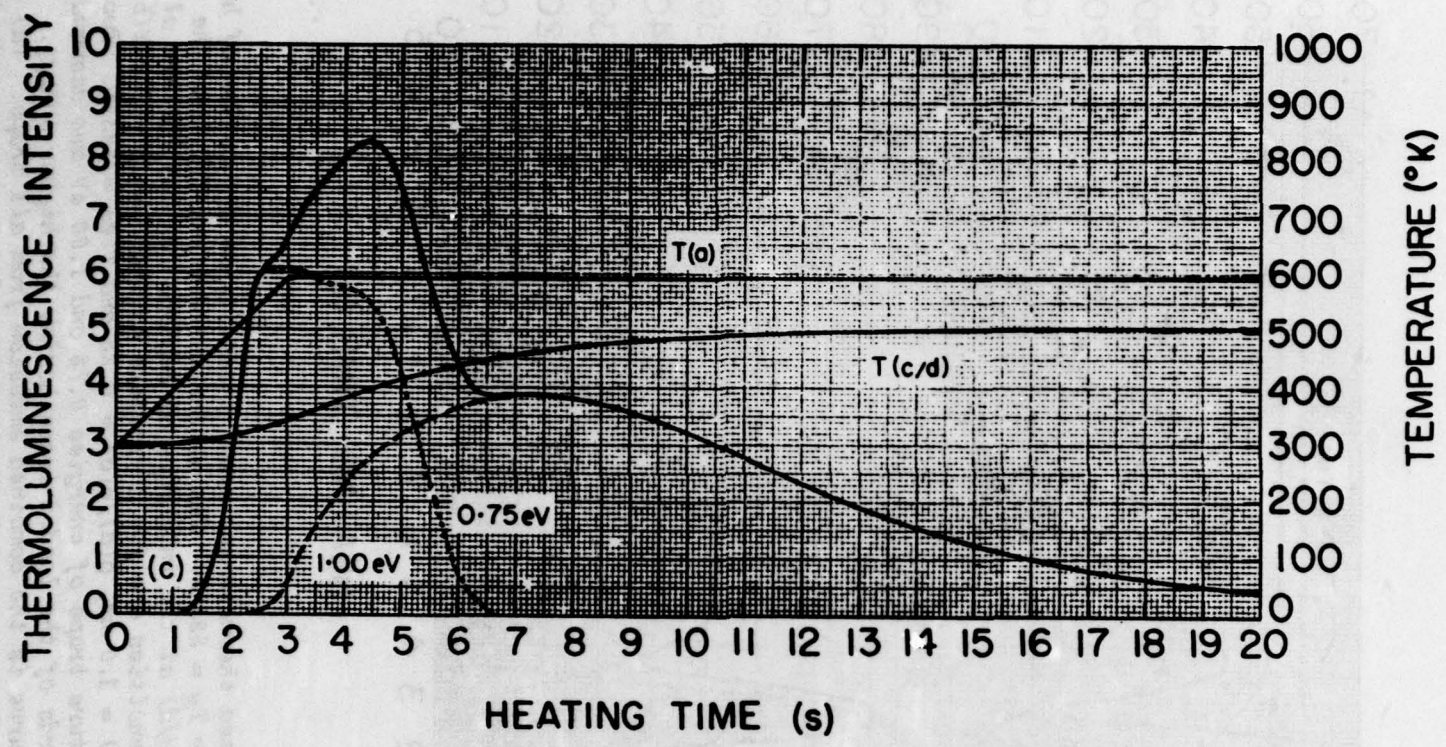

Fig. A5 (continued). (c) shows the calculated emission from a dosimeter with X(c) = 1.0 mm. Even for the two discrete energy traps there is considerable over lappping of the emission from the two traps. At 24 s there is still emission as the temperature T(c/d) has reached an equilibrium value of only 506°K and about 20% of the 1.00-eV traps remain filled.

Fig. 7, for comparable dimensions and measurement conditions. The model used here can thus be considered as a valid simulation of the combined neutron/gamma dosimeters and can be used to facilitate the choice of dosimeter parameters. As can be seen from Fig. A5 a compromise must be made in the choice of T_M, the heating time and the dosimeter thickness. Upper limitations are set on T_M by the decrease in mechanical support with increase in temperature of the dosimeter matrix (softening of the polyethylene) and by the increase in extraneous light from surfaces with increased temperature. For the instrument to be efficient as a field reader a heating cycle longer than 10 s is undesirable. Decreasing the matrix thickness, of course, decreases the dosimeter sensitivity, but from measurements reported in this report adequate sensitivity should be available from 0.25-mm dosimeters which can be read in less than 10 s with temperatures not exceeding 550°K.

A3. References

A1. D. Curie, Luminescence in Crystals, Methuen and Co. Ltd., London, 1963.

A2. J.R. Cameron, N. Sunthralingam, G.N. Kenney, Thermoluminescent Dosimetry, University of Wisconsin Press, Madison, 1968.

UNCLASSIFIED

Security Classification

DOCUMENT CONTROL DATA - R & D

(Security classification of title, body of abstract and indexing annotation must be entered when the overall document is classified)

1. ORIGINATING ACTIVITY

Defence Research Establishment Ottawa
National Defence Headquarters
Ottawa, Ontario Canada K1A 0Z4

2a. DOCUMENT SECURITY CLASSIFICATION: UNCLASSIFIED

2b. GROUP: N/A

3. DOCUMENT TITLE

Field Reader for a Combined Neutron/Gamma Thermoluminescent Dosimeter (U)

4. DESCRIPTIVE NOTES (Type of report and inclusive dates)

Technical Note

5. AUTHOR(S) (Last name, first name, middle initial)

McGowan, S

6. DOCUMENT DATE	7a. TOTAL NO. OF PAGES	7b. NO. OF REFS
Dec. 1976	36	6

8a. PROJECT OR GRANT NO.	9a. ORIGINATOR'S DOCUMENT NUMBER(S)
	TN 76-30
8b. CONTRACT NO.	9b. OTHER DOCUMENT NO.(S) (Any other numbers that may be assigned this document)

10. DISTRIBUTION STATEMENT

Unlimited distribution

11. SUPPLEMENTARY NOTES	12. SPONSORING ACTIVITY
	DLAEEM

13. ABSTRACT

An experimental model of a field reader to be used to interpret a combined neutron/gamma thermoluminescent dosimeter for military personnel has been designed and constructed. This instrument can operate from the 24-V battery of a military vehicle and can read dose to personnel in the range of 1 to 1000 rads. Satisfactory operation has been demonstrated and it has been shown that no serious limitations on the accuracy of the dosimetry measurements are introduced by the reader.

UNCLASSIFIED

DSIS
72-508

UNCLASSIFIED

Security Classification

KEY WORDS

DOSIMETER
THERMOLUMINESCENT
NEUTRON
GAMMA
DOSIMETER READER

INSTRUCTIONS

1. ORIGINATING ACTIVITY: Enter the name and address of the organization issuing the document.

2a. DOCUMENT SECURITY CLASSIFICATION: Enter the overall security classification of the document including special warning terms whenever applicable.

2b. GROUP: Enter security reclassification group number. The three groups are defined in Appendix 'M' of the DRB Security Regulations.

3. DOCUMENT TITLE: Enter the complete document title in all capital letters. Titles in all cases should be unclassified. If a sufficiently descriptive title cannot be selected without classification, show title classification with the usual one-capital-letter abbreviation in parentheses immediately following the title.

4. DESCRIPTIVE NOTES: Enter the category of document, e.g. technical report, technical note or technical letter. If appropriate, enter the type of document, e.g. interim, progress, summary, annual or final. Give the inclusive dates when a specific reporting period is covered.

5. AUTHOR(S): Enter the name(s) of author(s) as shown on or in the document. Enter last name, first name, middle initial. If military, show rank. The name of the principal author is an absolute minimum requirement.

6. DOCUMENT DATE: Enter the date (month, year) of Establishment approval for publication of the document.

7a. TOTAL NUMBER OF PAGES: The total page count should follow normal pagination procedures, i.e., enter the number of pages containing information.

7b. NUMBER OF REFERENCES: Enter the total number of references cited in the document.

8a. PROJECT OR GRANT NUMBER: If appropriate, enter the applicable research and development project or grant number under which the document was written.

8b. CONTRACT NUMBER: If appropriate, enter the applicable number under which the document was written.

9a. ORIGINATOR'S DOCUMENT NUMBER(S): Enter the official document number by which the document will be identified and controlled by the originating activity. This number must be unique to this document.

9b. OTHER DOCUMENT NUMBER(S): If the document has been assigned any other document numbers (either by the originator or by the sponsor), also enter this number(s).

10. DISTRIBUTION STATEMENT: Enter any limitations on further dissemination of the document, other than those imposed by security classification, using standard statements such as:

(1) "Qualified requesters may obtain copies of this document from their defence documentation center."

(2) "Announcement and dissemination of this document is not authorized without prior approval from originating activity."

11. SUPPLEMENTARY NOTES: Use for additional explanatory notes.

12. SPONSORING ACTIVITY: Enter the name of the departmental project office or laboratory sponsoring the research and development. Include address.

13. ABSTRACT: Enter an abstract giving a brief and factual summary of the document, even though it may also appear elsewhere in the body of the document itself. It is highly desirable that the abstract of classified documents be unclassified. Each paragraph of the abstract shall end with an indication of the security classification of the information in the paragraph (unless the document itself is unclassified) represented as (TS), (S), (C), (R), or (U).

The length of the abstract should be limited to 20 single-spaced standard typewritten lines; 7½ inches long.

14. KEY WORDS: Key words are technically meaningful terms or short phrases that characterize a document and could be helpful in cataloging the document. Key words should be selected so that no security classification is required. Identifiers, such as equipment model designation, trade name, military project code name, geographic location, may be used as key words but will be followed by an indication of technical context.


FILM
4